5-2011

A rearrangement of the Z chromosome topology influences the sex-linked gene display in the European corn borer, Ostrinia nubilalis

Jeremy A. Kroemer
United States Department of Agriculture

Brad S. Coates
United States Department of Agriculture, brad.coates@ars.usda.gov

Tyasning Nusawardani
Iowa State University

S. Dean Rider Jr.
Wright State University - Main Campus

Lisa M. Fraser
University of California - Davis

A rearrangement of the Z chromosome topology influences the sex-linked gene display in the European corn borer, Ostrinia nubilalis

Abstract
Males are homogametic (ZZ) and females are heterogametic (WZ) with respect to the sex chromosomes in many species of butterflies and moths (insect order Lepidoptera). Genes on the Z chromosome influence traits involved in larval development, environmental adaptation, and reproductive isolation. To facilitate the investigation of these traits across Lepidoptera, we developed 43 degenerate primer pairs to PCR amplify orthologs of 43 Bombyx mori Z chromosome-linked genes. Of the 34 orthologs that amplified by PCR in Ostrinia nubilalis, 6 co-segregated with the Z chromosome anchor markers kettin (ket) and lactate dehydrogenase (ldh), and produced a consensus genetic linkage map of ~89 cM in combination with 5 AFLP markers. The O. nubilalis and B. mori Z chromosomes are comparatively co-linear, although potential gene inversions alter terminal gene orders and a translocation event disrupted synteny at one chromosome end. Compared to B. mori orthologs, O. nubilalis Z chromosome-linked genes showed conservation of tissue-specific and growth-stage-specific expression, although some genes exhibited species-specific expression across developmental stages or tissues. The O. nubilalis Z chromosome linkage map provides new tools for isolating quantitative trait loci (QTL) involved in sex-linked traits that drive speciation and it exposes genome rearrangements as a possible mechanism for differential gene regulation in Lepidoptera.

Keywords
Z chromosome, Genetic map, Ostrinia nubilalis, Lepidoptera, Gene expression

Comments
This article is from *Molecular Genetics and Genomics*; 286 (2011); 37-56; doi: 10.1007/s00438-011-0624-1

Authors
Jeremy A. Kroemer, Brad S. Coates, Tyasning Nusawardani, S. Dean Rider Jr., Lisa M. Fraser, and Richard L. Hellmich

Mol Genet Genomics (2011) 286:37–56
DOI 10.1007/s00438-011-0624-1

ORIGINAL PAPER

A rearrangement of the Z chromosome topology influences the sex-linked gene display in the European corn borer, *Ostrinia nubilalis*

Jeremy A. Kroemer · Brad S. Coates · Tyasning Nusawardani · S. Dean Rider Jr. · Lisa M. Fraser · Richard L. Hellmich

Received: 25 August 2010 / Accepted: 16 April 2011 / Published online: 15 May 2011

Abstract Males are homogametic (ZZ) and females are heterogametic (WZ) with respect to the sex chromosomes in many species of butterflies and moths (insect order Lepidoptera). Genes on the Z chromosome influence traits involved in larval development, environmental adaptation, and reproductive isolation. To facilitate the investigation of these traits across Lepidoptera, we developed 43 degenerate primer pairs to PCR amplify orthologs of 43 *Bombyx mori* Z chromosome-linked genes. Of the 34 orthologs that amplified by PCR in *Ostrinia nubilalis*, 6 co-segregated with the Z chromosome anchor markers *kettin* (*ket*) and *lactate dehydrogenase* (*ldh*), and produced a consensus genetic linkage map of ~89 cM in combination with 5 AFLP markers. The *O. nubilalis* and *B. mori* Z chromosomes are comparatively co-linear, although potential gene inversions alter terminal gene orders and a translocation event disrupted synteny at one chromosome end. Compared to *B. mori* orthologs, *O. nubilalis* Z chromosome-linked genes showed conservation of tissue-specific and growth-stage-specific expression, although some genes exhibited species-specific expression across developmental stages or tissues. The *O. nubilalis* Z chromosome linkage map provides new tools for isolating quantitative trait loci (QTL) involved in sex-linked traits that drive speciation and it exposes genome rearrangements as a possible mechanism for differential gene regulation in Lepidoptera.

Keywords Z chromosome · Genetic map · *Ostrinia nubilalis* · Lepidoptera · Gene expression

Communicated by S. Hohmann.

J. A. Kroemer (✉) · B. S. Coates · R. L. Hellmich
USDA-ARS, Corn Insects and Crop Genetics Research Unit, Genetics Laboratory, Iowa State University, Ames, IA 50011, USA
e-mail: jkroemer@iastate.edu; Jeremy.Kroemer@ARS.USDA.GOV

T. Nusawardani
Department of Entomology, Iowa State University, Ames, IA 50011, USA

S. D. Rider Jr.
Department of Biochemistry and Molecular Biology, Wright State University, Dayton, OH 45435, USA

L. M. Fraser
Department of Microbiology, UC Davis, Davis, CA 95616, USA

Introduction

Females from the insect order Lepidoptera (butterflies and moths) are heterogametic with WZ sex chromosomes, whereas males of the same species have a ZZ pair of sex chromosomes (Traut and Marec 1997). Phenotypic traits controlled by loci on the Z chromosome in the domesticated silkworm, *Bombyx mori*, include cuticle density (loci *os*, sex-linked translucent, and *od*, distinct translucent), body shape (*e*, elongated), molting (*nm-s*, non-molting-s), larval maturity (*lm*, late maturity) and body color (*sch*, sex-linked chocolate) (Fujii et al. 2008). Genetic linkage maps of the *B. mori* Z chromosome (Nagaraja et al. 2005) have proven valuable in isolating the positions of *sch* (Miao et al. 2008) and *shaker* (*shkr*), which are linked to economically important male silking traits (Zhu et al. 2001), and behavioral traits, respectively (Duan et al. 2010). Among other species of Lepidoptera, the Z chromosome encodes the *period* (*per*) gene that governs clock and circadian periodicity in the silkmoth, *Antheraea pernyi* (Gotter et al. 1999), hybrid sterility factors in the Postman butterfly, *Heliconius melpomene* (Jiggins et al. 2001a), and ecological traits such as diapause duration and male

pheromone response in the European corn borer, *Ostrinia nubilalis* (Thomas et al. 2003; Dopman et al. 2005).

Diapause is a state of slowed development and physiological change (Palli et al. 1998) that is triggered by genetic factors in response to environmental cues including photoperiod and temperature (Hairston and Kearns 1995). Obligatory diapause has become fixed in populations due to selection within local environments, where for example, a univoltine ecotype of *O. nubilalis* predominates northern climates (Showers et al. 1975). In contrast, the majority of insects display facultative diapause as an adaptive strategy that allows for an increased number of generations under favorable conditions or the ability to enter a dormant state in an unfavorable environment (Liu et al. 2010). An increase in the number of generations per year can affect the ecology and evolution of a species (Hunter and McNeil 1997) such that genes influencing voltinism may be under selection during periods of climate change (Tobin et al. 2008; Altermatt 2010). Larval diapause traits are male sex-linked in *O. nubilalis* (Arbuthnot 1949; Showers et al. 1972; McLeod 1976). The univoltine trait is incompletely dominant and is linked to the *triosephosphate isomerase* (*tpi*) locus on the Z chromosome (Glover et al. 1992). The genes that regulate the univoltine phenotype in *O. nubilalis* are likely to be under positive selection in northern clines and may ensure over-wintering survival (Showers 1979), which reinforces genetic isolation from sympatric bivoltine ecotypes through incompatible breeding cycles (West-Eberhard 2003).

A second ecotype division within *O. nubilalis* is based upon female production and male response to the *E*11- and *Z*11-14:OAc-isomers of the pheromone Δ11-tetradecenyl acetate (Klun 1975). Females emit a blend of *E* and *Z* isomers under the control of the autosomal fatty acid reductase locus (Lassance et al. 2011) at blend ratios of 99:1 (E strain), 3:97 (Z strain), or 98:2 (Glover et al. 1987; Roelofs et al. 1987). Genes influencing long-range male pheromone perception are both autosomal and sex-linked (Roelofs et al. 1987; Lofstedt et al. 1989; Gould et al. 2010; Olsson et al. 2010). The autosomal pheromone perception loci regulate the development of alternative forms of the male pheromone receptor sensilla. The differences in male pheromone perception are associated with the macroglomerular complex (MGC) of male antennal lobes, where MGC morphology is indistinguishable between strains while the behavioral responses to pheromone stimulation are Z-linked and differ between E and Z moths (Karpati et al. 2008; Olsson et al. 2010). Pheromone perception generates a predictable electrochemical response through neurons connected to the MGC (Kanzaki et al. 2003). Chemical-derived neuroelectric signals display either large or small electrical spike amplitudes, with the sensilla being "tuned" to produce the larger amplitude signal in response to the strain-specific pheromone isomers (Roelofs et al. 1987). While corresponding behavioral changes are a probable catalyst for mating disruption and speciation (Sperling 1994), those responses are more difficult to characterize mechanistically (Ferveur et al. 1995). Although the genetic and molecular basis for Z chromosome-linked behavioral differences and other phenomena that drive speciation have yet to be fully characterized in *O. nubilalis*, male-influenced speciation in Lepidoptera was demonstrated in Postman butterfly (*H. melpomene*) ecotypes by the presence of hybrid sterility factors that are carried on the Z chromosome (Jiggins et al. 2001a). Such comparisons can be used to shed light on economically important Lepidoptera like *O. nubilalis*.

The genome sequence of *B. mori* displays substantial synteny with other Lepidoptera (Yasukochi et al. 2006; Pringle et al. 2007) making it an important tool for comparative genomics. The assembled *B. mori* Z chromosome sequence encompasses 20.4 Mb from five assembled scaffolds and is predicted to encode at least 655 genes (Yamamoto et al. 2006; Fujii et al. 2008). A corresponding genetic linkage map for the Z chromosome of *O. nubilalis* was previously assembled from 8 amplified fragment length polymorphisms (AFLPs), polymorphisms for *kettin* (*ket*), *lactate dehydrogenase* (*ldh*) and *tpi*, and a microsatellite marker (ma169) that were dispersed over an estimated 76 centi-Morgan (cM) distance (Dopman et al. 2005). That study confirmed that genes influencing the timing of larval post-diapause development (*pdd*) are genetically linked to the *tpi* locus (Roelofs et al. 1987), and indicated that the male behavior toward female pheromones is controlled by the male flight response (*resp*) quantitative trait locus (QTL) roughly 20 cM away from *tpi* (Dopman et al. 2005). The contribution of *resp* to the pre-mating barriers that reduce gene flow and that reinforce divergence of the E and Z moth strains is not fully understood (Dopman et al. 2010), but the current resolution of the Z chromosome map in *O. nubilalis* does not easily facilitate the isolation of specific genetic elements governing sex-linked traits in this species.

Using the *B. mori* Z chromosome scaffold assembly as a reference, we developed a pipeline for orthologous marker development among Lepidoptera for comparative genetic linkage mapping in *O. nubilalis*. Here, we present a genetic linkage map of the *O. nubilalis* Z chromosome assembled from 13 segregating molecular markers and present an empirical annotation of *O. nubilalis* Z chromosome loci using gene expression data across tissues and growth stages. Augmentation of the *O. nubilalis* Z chromosome linkage map with gene annotation data reveals the effects that chromosomal translocations may have on gene expression. This study demonstrates that the *B. mori* genome assembly provides a valuable entry point into genomic

research of Lepidoptera and offers new tools for mapping sex-linked traits in a model of speciation and ecotype divergence.

Materials and methods

O. nubilalis pedigrees and DNA extraction

Ostrinia nubilalis pupae were obtained from a laboratory colony of the bivoltine Z pheromone ecotype maintained at the USDA-ARS, Corn Insects and Crop Genetics Research Unit (CICGRU), Ames, IA. Three parental pairs were established from emerged adults (pedigrees 8-04, 8-05, and 8-09), and resulting F_1 progeny were reared on semi-meridic diet until pupation (Guthrie 1990). DNA was extracted and quantified from individual pupae within pedigrees by methods previously described (Coates et al. 2007). Total genomic DNA was also extracted from nine species of Lepidoptera (see Table 4) and *Diabrotica virgifera virgifera* (Coleoptera: Chrysomelidae), using methods described previously (Coates and Hellmich 2003).

Development of orthologous gene markers on the Z chromosome

The *B. mori* genome sequence, and gene and protein sequence models (build 2 v. 3) were, respectively, retrieved from the Kaikobase files integratedseq.txt.gz, glean_cds.txt.gz and glean_pro.txt.gz (http://sgp.dna.affrc.go.jp/pubdata/genomicsequences.html, files), in which chromosome 1 (Z) genes were identified by names within the file glean_cds_on_chr.gff. The National Center for Biotechnology Information (NCBI) EST database (dbEST) accessions for Lepidoptera were downloaded in FASTA format, and imported into a local searchable database using the program BioEdit (Hall 1999). The local database was queried with *B. mori* Z chromosome gene and protein sequences using the tblastx and blastx search algorithms, respectively (cutoffs: percent sequence similarity $\geq$ 60% and *E*-values $\leq 10^{-5}$), and the top 8 blast hits were retrieved for each search. Sequences were imported into the MEGA 4.0 software package sequence alignment application (Tamura et al. 2007), and multiple sequence alignments were made with the ClustalW algorithm using default parameters (gap opening penalty 15, gap extension penalty 6.66, weight matrix IUB with a transition weight of 0.5) and the *B. mori* gene models to "guide" the alignment. Physical distances between genes were estimated with reference to the *B. mori* Z chromosome sequence scaffolds (Duan et al. 2010). Primer3 (Rozen and Skaletsky 2000) was used to design degenerate oligonucleotide primers that would anneal at sites with $\geq$80% homology across at least 4 putative orthologous lepidopteran genes, and to generate predicted products with 1 or 2 introns (Table 1). All primers were synthesized by Integrated DNA Technologies (Coralville, IA).

Orthologous genomic fragments were PCR amplified from $\sim$25 ng of DNA in reactions that used 1.5 mM $MgCl_2$, 50 µM dNTPs, 3.0 pmol of a degenerate primer pair (Table 1), 2 µl 5× thermal polymerase buffer (Promega, Madison, WI), and 0.15 U *Taq* DNA polymerase (Promega, Madison, WI) in a 10 µl reaction volume. Reactions were then cycled using the following parameters: 96°C, 2 min initial denaturation; 95°C, 30 s cycle denaturation; 55°C, 45 s cycle annealing; 72°C, 2 min cycle elongation; 72°C, 10 min final elongation; 4°C, hold. All PCR amplified fragments were separated on 1.5% agarose gels. PCR products from *O. nubilalis* females were purified using Gel/PCR DNA fragment extraction kits (IBI Scientific, Peosta, IA), cloned into pGEM-T (Promega, Madison, WI), and sequenced (Coates et al. 2010). *Ostrinia nubilalis* sequences were queried against the glean_cds.txt and glean_pro.txt files using tblastx and tblastn algorithms, aligned in MEGA 4.0 (Tamura et al. 2007) as described previously, and putative substitution mutations within restriction endonuclease sites were identified manually.

Comparative mapping of the Z chromosome

The segregation of predicted mutations (Table 2) among progeny from pedigrees 8-04, 8-05, and 8-09 were detected as described by Coates et al. (2008). All restriction enzymes were purchased from New England Biolabs (Ipswich, MA). Genomic DNA for parents and F_1 progeny from pedigrees 8-04, 8-05, and 8-09 were PCR amplified and single nucleotide polymorphism (SNP)-based genotypes were revealed using diagnostic fragment patterns (Table 2) with the co-occurrence of alleles A_1 and A_2 designated as heterozygotes, A_1A_2. Amplified fragment length polymorphism (AFLP) markers were generated for *O. nubilalis* pedigree 8-04. Approximately 0.5 µg of genomic DNA was digested with *Eco*RI and *Mse*I, ligated to adapters, and pre-amplified using core adapter primers as described (Vos et al. 1995). Thirty-two different combinations of selective *Eco*RI and *Mse*I primer pairs were used for amplification of AFLP markers in individual 10 µl reactions as described previously (Vos et al. 1995), except that selective *Mse*I primers were multiplexed with two selective *Eco*RI primers that were labeled with IRDye-700 or IRDye-800 (Table 3, LiCor, Lincoln, NE). AFLP products were diluted 1:4 with deionized water, to which 8 µl stop/loading buffer was added (LiCor, Lincoln, NE). Samples were heat denatured at 95°C for 10 min and snap chilled on ice for 10 min. Samples (1 µl) were then loaded into wells of a 0.2 cm 6.5% denaturing polyacrylamide gel

Table 1 Gene-specific and degenerate DNA primers designed from lepidopteran ESTs and the *B. mori* chromosome 1 (Z) scaffold for mapping the Z chromosome in *O. nubilalis*

Bombyx mori Z chromosome gene	*Bombyx mori* SilkDB Accession #	Degenerate primers	Gene-specific primers (*O. nubilalis*)	*Bombyx mori* Z chromosome gene	*Bombyx mori* SilkDB Accession #	Degenerate primers	Gene-specific primers (*O. nubilalis*)
Gene 1: Oligopeptide transporter	BGIBMGA000496-TA	ZG1-OP-FW: TTTAAATCT GGAGCWGTSTACAC		Gene 23: Ribosomal protein L36a	BGIBMGA001991-TA	ZG23RPFW: CTGCGAA ARGGSCACAARAC	
		ZG1-OP-RV: ACCGATTGT ARTACWGACTTCAT				ZG23RPRV: CTCCATW GCYCTCTTCTCATA	
Gene 2: Hypothetical protein 1	BGIBMGA000503-TA	ZG2-H1-FW: CTTGTGCTG GCAGTYGARCARGA		Gene 24: ATP-binding cassette	BGIBMGA002004-TA	ZG24ATFW: CTTGAAC GGWGTWTGYACSAA	
		ZG2-H1-RV: TTCAATTTC CAYTCCCAASCCAT				ZG24ATRV: GAGACCYT GWGCMACCAT	
Gene 3: mRNA binding protein	BGIBMGA000516-TA	ZG3-mB-FW: CACCCAAT GGCKATGATGTCKAC	G3 GSP FW: CTCTGCTCC AAACGTCCCAG	Gene 25: Laminin A	BGIBMGA002018-TA	ZG25LAFW: ATGGGMA ACTCMCCYCGYCC	
		ZG3-mB-RV: ATAATCGC GCCCACRGCRTTRTT	G3 GSP RV: GCACTGTTT TATCTCGTTCCTAC			ZG25LARV: CGTAGCC KAACRTTGGTKGC	
Gene 4: Cuticular protein	BGIBMGA000520-TA	ZG4-CP-FW: TTCGTGGT WCTCGCCTGTGTGGC	G4 GSP FW1: CAGCTACG GAGCTCCGTCCGC	Gene 26: Glucose transporter 1	BGIBMGA002023-TA	ZG26GTFW: ATGTAYA TMTCGGARATMGC	
		ZG4-CP-RV: CCTTTTGGG TTTGRTAYTTGATGAAGTA	G4 GSP RV: GTATACGAG GGTCTTCTCTTC			ZG26GTRV: GCCTCG CYTCYTCYTCCCA	
Gene 5: DNA-binding/C2H2 Zinc finger	BGIBMGA000521-TA	ZG5-H2-FW: CATATGCG TCGRCACACSGG		Gene 27: Tubulin alpha	BGIBMGA002103-TA	ZG27TAFW: CCTACA GTAGTRGATGAGGT	
		ZG5-nH-RV: TCACCGGTG TGAGATCKYCGRTG				ZG27TARV: TCGAAGCA MGCRTTGGTGAT	
Gene 6: Hypothetical protein 3	BGIBMGA000523-TA	ZG6-H3-FW: CCGCATATC ACGTGGTWYAARGA	G6 GSP FW: GACGGGGT TGAGATATTTGCG	Gene 28: Shaker potassium channel	BGIBMGA003851-TA	ZG28SPFW: CGGAACGAR TACTTCTTCGA	G28 GSP FW: CCGACACC ACCGCCACAACAC
		ZG6-H3-RV: GTAGCTGGA TCGATYTCGATYTT	G6 GSP RV: ATCGATTTC GATTTTGGACTTGAC			ZG28SPRV: CTTCAGCG AAGTACACCGC	G28 GSP RV: GCGACTGC CGCTGCTCTCCG
Gene 7: Cold shock protein	BGIBMGA000526-TA	ZG7-YB-FW: GTTCAACGTC AAGAGYGGATATGG		Gene 29: Ser-Thr protein kinase	BGIBMGA003858-TA	ZG29STFW: AAGGCCAC CAARGCYAARGT	
		ZG7-YB-RV: TCATCTCCYY GTGCACCCCC				ZG29STRV: GGAATTCAG TYTCYTTYTGSGC	
Gene 8: Zn metalloprotease	BGIBMGA000529-TA	ZG8-ZM-FW: AACGGCTCG GAGGHTGGC		Gene 30: Leucine zipper transcription factor	BGIBMGA003874-TA	ZG30PDFW: GAGCTGAA RCCRCARCC	
		ZG8-ZM-RV: ATATCGACC ATGTASTCRTARTA				ZG30PDRV: GGCYGC CATRTTGTTCTT	
Gene 9: Peroxidasin	BGIBMGA000553-TA	ZG9PtFW: ACGCATATGR YTATGCARTGGGG		Gene 31: Coatomer protein subunit	BGIBMGA003892-TA	ZG31CPFW: CAYACS CATTAYGTRATGCA	G31 GSP FW: CCGCCGT GGTAGTAGTCGAC
		ZG9PtRV: CCAAAGCGAA RAGCAGCDGTKGC				ZG31CPRV: CACATGTC TTRTTYTGRTARTCCCA	G31 GSP RV: CGAATCC TYTAGGCTGCAC
Gene 10: Tyrosine hydroxylase	BGIBMGA000563-TA	ZG10ThFW: TGGCCTTC CGTGTHTTCCA		Gene 32: L-Lactate dehydrogenase	BGIBMGA012336-TA	ECB_ldhF: GGCTCCGG CACCAACCTGGACTC	
		ZG10ThRV: TCTTGTGAGA ATTGRGCGAAGCT				ECB_ldhR: CGTAGGCGC TCTTCACCACCATCTCA	
Gene 11: Paramyosin	BGIBMGA000612-TA	ZG11PmFW: CGAGGAAA TCCGKCGCAARTAC	G11 GSP FW: ATCTTCCT TATTGCGTACCA	Gene 33: DNA-binding protein D-ETS-3	BGIBMGA012229-TA	ZG33DBFW: GACAAATMC ARCTRTGGCA	G33 GSP FW: CTGAGTG TAAGTATAACTGG
		ZG11PmRV: TTTGCCTTC TCCARRTCRATGAT	G11 GSP RV: GCATTCAG GAGCAGGAGGA			ZG33DBRV: CTCATGAAY ARGTCGCTYTG	G33 GSP RV: GAACACA ATGATACGTTTAAC
Gene 12: MiniParamyosin	BGIBMGA000613-TA	ZG12mPFW: GCATCTGCA TGARGARCARGA	G12 GSP FW: ATGCTCGT GACGTGAGTTTCCGC	Gene 34: CCR4-NOT complex subunit	BGIBMGA012230-TA	ZG34CTFW: CGCATTGG AYSCKGAYGA	
		ZG12mpRV: GCGGCTTCC AATTCRCKYTGGAA	G12 GSP RV: CCTCTTGTA GATGTTGACCTTC			ZG34CTRV: CTTCTTGACK GGCMAKYTT	

Table 1 continued

Bombyx mori Z chromosome gene	*Bombyx mori* SilkDB Accession #	Degenerate primers	Gene-specific primers (*O. nubilalis*)	*Bombyx mori* Z chromosome gene	*Bombyx mori* SilkDB Accession #	Degenerate primers	Gene-specific primers (*O. nubilalis*)
Gene 13: FK506-binding protein	BGIBMGA000619-TA	ZG13FkFW: ACCAACG TCTTCAARGARATCGA	G13 GSP FW: GACTTCAC TATCATCGGAAGAG	Gene 35: GTP-binding protein	BGIBMGA012295-TA	ZG35GBFW: GAGCTTAARG CWGTYAARTATGT	G35 GSP FW: ACAAGAA AAGATTACAGTAACTG
		ZG13FkRV: GGCGGGAA CCATYTGCTTCTT	G13 GSP RV: CAGTTTCC GCTTTCTGCAGG			ZG35GBRV: AGTATRGCCT CRTCRAAYAC	G35 GSP RV: ATGTTGTAG TGTTCTGCTCTCAC
Gene 14: Kettin	BGIBMGA000622-TA	ECBketF: TGAAATCCCG GAACCAGTAACA		Gene 36: Fibronectin	BGIBMGA012306-TA	ZG36AFFW: CAACGACAA GARMGKGCDAT	
		ECBketR: TTGAGGTGAG TAGTGAAAATAGGAG				ZG36AFRV: GTTTATTCTT SACRCTGGGGAA	
Gene 15: Bestrophin	BGIBMGA000628-TA	ZG15BsFW: CTATTCGAG TCCTGARRCRGGC		Gene 37: ADP-ribosylation factor	BGIBMGA012325-TA	ZG37ARFW: GGTCGGA CTYGAYAAYGC	
		ZG15BsRV: CGTCCGGTGT RGGWATRCG				ZG37ARRV: TTGTGTAGT ARGTRTTCCAYGC	
Gene 16: Citrate synthase	BGIBMGA000672-TA	ZG16CsFW: CACTACCCGA RGGTCTBTTCTGG		Gene 38: Amino acid transporter (H-coupled)	BGIBMGA012328-TA	ZG38PCFW: TGCCTTK GARGGWATYGG	G38 GSP FW: CCTTGACGT GATAGTGATC
		ZG16CsRV: CCGAGAAC TGWGACATSGGRTG				ZG38PCRV: CCATGGGCA CGTAGAAYTG	G38 GSP RV: GAGGCTGT ATGTGAACAG
Gene 17: Glutamine synthetase	BGIBMGA000680-TA	ZG17GsFW: TATGGAACT TCGAYGGYAGYTC		Gene 39: F-box, WD40 domain protein	BGIBMGA012355-TA	ZG39FBFW: CACGCTYA TSGGYCAYCA	
		ZG17GsRV: GAACTCCCA CTGKGAMGGCAT				ZG39FBRV: AGTTTCGTC TCCTCVGTKCC	
Gene 18: Calponin-like	BGIBMGA000683-TA	ZG18BPFW: TGACGGTCA RGTDCTDCARAA		Gene 40: Hypothetical protein 6	BGIBMGA013327-TA	ZG40H6FW: ATGAGTGC TCCAGCACC	
		ZG18BPRV: AACAACGCR TCRAAYGCRTC				ZG40H6RV: GCGAGTTTM GGYGCSGTGA	
Gene 19: Neuralized-bluestreak	BGIBMGA000698-TA	ZG19NBFW: TTATCCCGA ARTGGGCYGG		Gene 41: Hypothetical protein 7	BGIBMGA000699-TA	ZG41H7FW: AAGTGGGCR WTRGTYGARCA	
		ZG19NBRV: GGTAATAGC CCAMGTKCCTGA				ZG41H7RV: TGTCTACTAR CAKYTCRTGRTC	
Gene 20: Catalase	BGIBMGA000701-TA	ZG20CAFW: ACTTTGAAG TWACYCATGAYAT		Gene 42: Suppressin	BGIBMGA002019-TA	ZG42DEFW: GTACACCC CBAGYGARTTYGA	G42 GSP FW: AAACATG GTAGGTCAGCAT
		ZG20CARV: ATGCAATT TGYTCMACTTCRGC				ZG42DERV: TTCGCTTTC TTTTRTATGGAGTRAA	G42 GSP RV: AGCTCTCT GTGGGAGAGCTTC
Gene 21: Acyl-CoA dehydrogenase	BGIBMGA000715-TA	ZG21ADFW: CATGCT GGCMGAYATGGC		Gene 43: Triose phosphate isomerase	BGIBMGA000559-TA	ECBtpi_for1A: AGATGTCA AAATTCAACTCAG	
		ZG21ADRV: CCGAATAT CTGKACSGCRTC				ECBtpi_rev5: AGCACCCT TCGGCACTT	
Gene 22: Hypothetical protein 4	BGIBMGA002001-TA	ZG22HPFW: ATCCACTA YGTCMGRGAGCA	G22 GSP FW: CAGATGAA GTAGGTACCCGCC				
		ZG22HPRV: CGATATAAG YTCYTCCARGTC	G22 GSP RV: ATCATTTAC AGTATGTAGCC				

Table 2 Single nucleotide polymorphism (SNP) and PCR fragment length polymorphism markers from *O. nubilalis* detected following amplification and restriction enzyme (RE) digestion of PCR products

Ortholog marker	SilkDB *B. mori* gene ID	RE digest	Fragment sizes for alleles (bp)	
			A_1	A_2
G02	BGIBMGA000503-TA	*Hinf*I	800	600, 120, 80
G04	BGIBMGA000520-TA	*Msp*I	100	50, 50
G11	BGIBMGA000612-TA	*Dra*I	200	150, 50
G12	BGIBMGA000613-TA	*Hpy*188I	500	250, 250
G13	BGIBMGA000619-TA	*Ssp*I	500	300, 200
G14 (*ket*)	BGIBMGA000622-TA	*Rsa*I	600, 200, 50	400, 200, 100, 100, 50
G23	BGIBMGA001991-TA	PCR	850	700
G28 (*shkr*)	BGIBMGA003851-TA	*Hpy*CH4IV	700, 300, 50	700, 150, 150, 50
G31	BGIBMGA003892-TA	*Msp*I	700, 70	500, 120, 100, 50
G32 (*ldh*)	BGIBMGA012336-TA	*Alu*I	150	100, 25, 25
G33	BGIBMGA012229-TA	*Cfo*I	550, 75, 50	500, 125, 50
G38	BGIBMGA012328-TA	PCR	700	400

Designations for alleles A_1 and A_2 are given in base pair (bp)

Table 3 Oligonucleotide primer pairs used for PCR amplification of AFLP markers in *O. nubilalis* pedigree 8-04 (*Eco*RI-CORE1 = 5′-GAC TGC CGT ACC AAT TC-3′ Mse-CORE2 = 5′-CGA TGA GTC CCT GAG TAA-3′)

MP	*Eco*RI primer IRDye-700	*Eco*RI primer IRDye-800	*Mse*I primer (unlabeled)
01	*Eco*RI-CORE1 + ACA-700	*Eco*RI-CORE1 + ACT-800	*Mse*I-CORE2 + TG
02	*Eco*RI-CORE1-AAG700	*Eco*RI-CORE1 + AGC-800	*Mse*I-CORE2 + TG
03	*Eco*RI-CORE1 + AAC-700	*Eco*RI-CORE1 + ACG-800	*Mse*I-CORE2 + GA
04	*Eco*RI-CORE1 + AAG-700	*Eco*RI-CORE1 + AGC-800	*Mse*I-CORE2 + GA
05	*Eco*RI-CORE1 + AAG-700	*Eco*RI-CORE1 + AGC-800	*Mse*I-CORE2 + GT
06	*Eco*RI-CORE1 + AAG-700	*Eco*RI-CORE1 + AGC-800	*Mse*I-CORE2 + CG
07	*Eco*RI-CORE1 + ACC-700	*Eco*RI-CORE1 + AGG-800	*Mse*I-CORE2 + ACG
08	*Eco*RI-CORE1 + AAG-700	*Eco*RI-CORE1 + AGC-800	*Mse*I-CORE2 + ACG
09	*Eco*RI-CORE1 + AAC-700	*Eco*RI-CORE1 + ACG-800	*Mse*I-CORE2 + CAT
10	*Eco*RI-CORE1 + ACC-700	*Eco*RI-CORE1 + AGG-800	*Mse*I-CORE2 + CAT
11	*Eco*RI-CORE1 + ACA-700	*Eco*RI-CORE1 + ACT-800	*Mse*I-CORE2 + CAT
12	*Eco*RI-CORE1 + AAG-700	*Eco*RI-CORE1 + AGC-800	*Mse*I-CORE2 + CAT
13	*Eco*RI-CORE1 + ACA-700	*Eco*RI-CORE1 + ACT-800	*Mse*I-CORE2 + CTA
14	*Eco*RI-CORE1 + AAG-700	*Eco*RI-CORE1 + AGC-800	*Mse*I-CORE2 + CTA
15	*Eco*RI-CORE1 + ACA-700	*Eco*RI-CORE1 + ACT-800	*Mse*I-CORE2 + GAG
16	*Eco*RI-CORE1 + AAG-700	*Eco*RI-CORE1 + AGC-800	*Mse*I-CORE2 + GAG

(including 1 µl of the LiCor 50–700 bp molecular size standard used for size comparison). Fragment separations were performed at 1500 V, 40 mA, and 45°C for 3.5 h on a Model 4300 DNA Analyzer (LiCor, Lincoln, NE). TIF images were collected from IRDye-labeled fragment migration rates using the SAGA^{MX} software suite. Marker bins ± 1 bp of estimated marker sizes were determined by comparison to the 50–700 bp molecular size standards and marker data were exported in tab-delimited format.

Co-dominant SNP and dominant AFLP-based markers were coded for MAPMAKER 3.0 (Lincoln et al. 1992) wherein the presence of an AFLP band or a SNP heterozygote in the F_1 progeny from pedigree 8-04 was coded as an "H", and the absence of an AFLP band or a SNP homozygote was coded as an "A". This was possible in the F_1 generations because recombination only occurs during male meiosis and not during female oogenesis in Lepidoptera. AFLP and SNP data were tested using Chi-square analyses (χ^2, P value cutoff > 0.05) to identify significant deviations from the expected 1:1 Mendelian ratio for segregating markers among F_1 progeny. Only SNP data were generated for pedigrees 8-05 and 8-09 because genomic

DNA resources were not of sufficient quantity to perform AFLP analyses. Linkage associations among segregating markers were determined independently for each pedigree (cutoffs: LOD $\geq$ 3.0 and $r \leq 0.40$). Independent associations were then ordered based upon the minimum sum of adjacent recombination fractions (SARF) and tested by Log-likelihood estimates (Falk 1992). All possible marker orders were constructed and marker order was established using the smallest estimated Kosambi map distances and logarithm of the likelihood for each map length [map Log-likelihood]. A consensus map of 13 Z chromosome-linked markers was generated using MergeMap (Wu et al. 2008) with data collected from pedigrees 8-04, 8-05, and 8-09.

Bridging *O. nubilalis* Z chromosome genetic and physical maps

A portion of the *O. nubilalis* bacterial artificial chromosome (BAC) library, OnB1, comprising an approximate fourfold genome coverage was screened via PCR of clone superpools (SPs) and rowpools (RPs) as previously described with the 43 Z chromosome marker primer pairs (Coates et al. 2009). Positive OnB1 BAC clones were validated for haplotype inserts by direct sequencing (Coates et al. 2009).

Expression of *O. nubilalis* Z chromosome orthologs

Life cycle samples

Three replicates of each of the following *O. nubilalis* life stages were collected: whole embryonic egg masses (4/replicate), pre-emergent black-head egg masses (4/replicate), second instar larvae (30/replicate), third instar larvae (10/replicate), fourth instar larvae (2/replicate), fifth instar larvae (1/replicate), pupae (1/replicate), male adults (1/replicate), and female adults (1/replicate). Samples were immersed in liquid nitrogen, ground into a powder, and then total RNA isolated in 500 µL Trizol Reagent according to the manufacturer's protocol (Invitrogen, Carlsbad, CA).

Tissue-specific samples

Premolt fourth and fifth instar *O. nubilalis* larvae were anesthetized by immersion in ice-cold phosphate buffered saline (PBS: 137 mM NaCl, 2.7 mM KCl, 4.3 mM $Na_2HPO_4 \times 7H_2O$, 1.4 mM KH_2PO_4, pH 7.4) for 20 min. Hemocytes (HC) were collected from 40 individuals for both fourth and fifth instar larvae by cutting the first proleg with surgical scissors and bleeding into 200 µL of ice-cold PBS, centrifuging at 800×*g* for 5 min, and washing 3 times with 1 mL of ice-cold PBS. Heads (Hd), fat body (FB), digestive tracts including Malphigian tubules and gut (Gu), and remaining carcass (Ca) tissues including muscle, trachea, nerve cord, and epidermis were dissected into 500 µL ice-cold PBS and washed in the same manner as HC samples. Following washes, total RNA was isolated as described previously.

Oligo-dT primed synthesis of cDNA was performed with the SMART IV cDNA Library Construction Kit (Clontech, Mountain View, CA) for all replicated *O. nubilalis* total RNA pools using 3 µg of total RNA per synthesis reaction (Coates et al. 2008). The resulting cDNA was diluted 1:25 with nuclease-free water and 1 µL was used as template in RT-PCR reactions with SNP marker primers (Table 1). Amplified products were separated on 1.5% agarose gels as described above. The expression of *O. nubilalis* Z chromosome orthologs was compared to raw microarray data from *B. mori* fifth instars (Xia et al. 2007) downloaded from SilkDB (Duan et al. 2010) as tab-delimited text. The presence or absence of gene expression was scored using majority rules criteria for each *O. nubilalis* ortholog, and compared to *B. mori* microarray data that was Log-transformed and grouped using the Gene Cluster 3.0 program (de Hoon et al. 2004). *Bombyx mori* heatmaps were generated using the Java Treeview program (Saldanha 2004).

Results

Development of orthologous gene markers on the Z chromosome

The 43 degenerate primer pairs (Table 1) PCR amplified putative *B. mori* Z chromosome orthologs from 10 species of Lepidoptera and one species of Coleoptera with a mean of 28.3 ± 3.6 markers per species in the Lepidoptera and 27.5 ± 4.2 overall (Table 4). Of the 34 primer pairs amplifying products from random *O. nubilalis* individuals, ~75% produced consistent PCR products among individuals within F_1 pedigrees from the laboratory colony. Amplified products from F_1 pedigrees were validated as Z chromosome orthologs following query of sequence generated from markers G04, G06, G11, G12, G14 (*ket*), G20, G23, G28 (*shkr*), G31, G32 (*ldh*), and G43 (*tpi*) against the *B. mori* gene models (top blastn and tblastx hits in Table 5). In contrast, low or no identity was shown at sequence tags for markers G03, G10, G13, G22, G33, G37, G38, or G42, and may be due to a high proportion of sequence from intronic regions (Table 5). All marker sequences collected from *O. nubilalis* were deposited in GenBank (accessions in Table 5).

Table 4 Test of degenerate Z chromosome primer pairs against a panel of 10 lepidopteran pest species and western corn rootworm

Z gene marker	*ket*																											*shkr*				*ldh*																*tpi*
Pest	1	2	3	4	5	6	7	8	9	10	11	12	13	14	15	16	17	18	19	20	21	22	23	24	25	26	27	28	29	30	31	32	33	34	35	36	37	38	39	40	41	42	43
European corn borer (*Ostrinia nubilalis*)	N	+	+	+	N	+	N	+	+	+	+	+	+	+	N	+	N	N	+	+	+	+	+	N	+	+	+	+	+	+	+	+	+	+	+	+	+	+	+	N	N	+	+
Asian corn borer (*Ostrinia furnicalis*)	N	N	N	+	N	N	N	N	N	+	+	N	+	+	N	N	+	N	N	+	+	N	+	+	+	+	+	+	N	+	+	+	+	+	+	+	+	+	+	N	N	+	+
Rice borer (*Chilo suppressalis*)	+	+	+	+	+	N	N	+	N	+	N	N	N	N	N	N	+	N	+	+	+	+	+	N	+	+	+	+	+	+	+	N	N	+	N	+	N	+	+	+	+	N	N
Indianmeal moth (*Plodia interpunctella*)	N	N	+	+	+	+	+	N	+	N	+	+	+	+	N	+	+	+	+	N	N	+	+	N	+	+	+	+	N	+	+	N	+	N	N	+	+	+	N	+	+	N	+
Mediterranean flour moth (*Ephestia kuehniella*)	+	+	+	+	+	N	N	+	+	+	+	+	N	+	+	+	+	N	+	N	+	N	+	N	N	+	N	+	N	+	N	N	N	+	N	+	N	+	+	+	+	+	N
Black cutworm (*Agrotis ipsilon*)	N	+	+	+	+	+	+	N	+	+	+	+	+	N	+	+	+	+	+	+	+	N	+	+	+	+	+	+	+	+	+	N	+	N	+	N	+	+	+	+	N	+	N
Western bean cutworm (*Striacosta albicosta*)	N	N	+	+	N	N	N	N	N	+	+	+	N	N	N	+	+	+	+	N	N	+	+	+	N	N	+	N	+	+	+	N	+	+	+	+	N	+	+	+	+	N	N
Sugarcane borer (*Diatraea saccharalis*)	+	N	N	N	+	+	+	N	+	N	+	N	+	N	N	+	+	N	+	+	+	+	+	+	N	N	+	+	N	+	+	+	+	+	N	+	N	+	+	+	N	N	N
Lesser cornstalk borer (*Elasmopalpus lignosellus*)	+	+	+	+	N	+	N	N	+	N	+	+	+	+	+	+	+	+	+	+	+	N	+	N	N	N	+	N	N	+	+	+	+	+	+	+	+	+	+	+	N	N	+
Greater wax moth (*Galleria mellonella*)	N	+	+	+	+	+	N	N	+	N	+	N	N	N	+	+	+	+	N	N	N	N	+	N	+	+	+	+	+	+	+	+	+	+	+	N	+	+	+	N	N	N	N
Western corn rootworm (*Diabrotica virgifera virgifera*)	N	+	N	N	+	N	+	+	+	+	+	N	N	N	N	+	+	N	+	+	N	+	N	+	+	+	N	N	+	+	N	N	+	N	N	N	N	N	+	N	+	N	N

ket, *shkr*, *ldh*, and *tpi*: visual landmarks for the behavioral *shaker* gene and other genes previously mapped (Dopman et al. 2005) to the *O. nubilalis* Z chromosome, *N* amplification reactions yielded no single or consistent PCR product

Table 5 Linear order of Z chromosome (chr 1) linked genes in *B. mori*, and the results of *O. nubilalis* pedigree screens, PCR sequencing, and BAC library screening with validated Z gene markers

B. mori chr 1 (Z) gene order	*B. mori/O. nubilalis* Z gene marker	*B. mori* SilkDB Accession #	*B. mori* SilkDB scaffold	*B. mori* position start	*B. mori* position end	*O. nubilalis* polymorphic pedigrees	*O. nubilalis* PCR sequence (bp)	*O. nubilalis* Genbank Accession	*O. nubilalis* SilkDB match	*O. nubilalis* E value	*O. nubilalis* current Z Assembly	*O. nubilalis* positive BAC clone	*O. nubilalis* BAC sequence (bp)	*O. nubilalis* Genbank Accession	*O. nubilalis* SilkDB match	*O. nubilalis* E value
1	*Gene 42: Suppressin*	*BGIBMGA002019-TA*	*2210*	*2453089*	*2459028*		*230*	HQ116678	*No significant match*		*Predicted autosomal linkage*					
2	*Gene 25: Laminin A*	*BGIBMGA002018-TA*	*2210*	*2489754*	*2548751*						*Predicted autosomal linkage*	*64J21, 76A15*				
3	*Gene 22: Hypothetical protein 4*	*BGIBMGA002001-TA*	*2210*	*4688480*	*4695395*		*459*	HQ116670	*No significant match*		*Predicted autosomal linkage*	*75B13, 75F20*				
4	*Gene 23: Ribosomal protein L36a*	*BGIBMGA001991-TA*	*2210*	*4988669*	*4991978*	*8-04*	*472, 628*	HQ116671, HQ116672	*BGIBMGA001991-TA*	*4.00E−10*	*NOT Z-linked in O. nubilalis pedigrees*	*48G22*	*738*	*HQ116692*	*BGIBMGA001991-TA*	*1.00E-21*
5	Gene 11: Paramyosin	BGIBMGA000612-TA	1690	5986870	5995315	8-09	405	HQ116665	BGIBMGA000612-TA	8.00E−26	BAC Linked to G12, Z-linked in *O.nubilalis* pedigrees	64B04, 47B01	353	HQ116685	BGIBMGA000612-TA	6.00E−15
6	Gene 12: MiniParamyosin	BGIBMGA000613-TA	1690	5996191	6001432	8-09, 8-05	623	HQ116666	BGIBMGA000613-TA	2.00E−59	BAC Linked to G11, Z-linked in *O.nubilalis* pedigrees	64B04	550	HQ116686	BGIBMGA000613-TA	6.00E−56
7	Gene 13: FK506-binding protein	BGIBMGA000619-TA	1690	6438135	6440160	8-09, 8-05	642	HQ116667	No significant match		Z-linked in *O.nubilalis* pedigrees	44A08, 44F07				
8	Gene 14: Kettin	BGIBMGA000622-TA	1690	6505696	6533895	8-05, 8-04	692	HQ116668	BGIBMGA000622-TA	1.00E−21	Z-linked in *O.nubilalis* pedigrees	03E15, 77C21	694	HQ116687	BGIBMGA000622-TA	8.00E−69
9	Gene 10: Tyrosine hydroxylase	BGIBMGA000563-TA	1690	8795736	8803023		696	HQ116664	No significant match		Predicted Z-linkage in *O. nubilalis*	75E15, 75E22				
10	Gene 43: Triosephosphate isomerase	BGIBMGA000559-TA	1690	9023681	9026446		319	HQ116677	BGIBMGA000559-TA	5.00E−18	Z-linked in *O.nubilalis* pedigrees (Dopman et al. 2005)	63H07	Coates et al. (2009)			
11	Gene 16: Citrate synthase	BGIBMGA000672-TA	1690	9370203	9385213						Predicted Z-linkage in *O. nubilalis*	52L07	602, 753	HQ116688, HQ116689	BGIBMGA000672-TA	1.00E−10
12	Gene 20: Catalase	BGIBMGA000701-TA	1690	10876713	10879032		674	HQ116669	BGIBMGA000701-TA	3.00E−70	BAC Linked to G6, predicted Z-linkage in *O. nubilalis*	66E06	538	HQ116690	BGIBMGA000701-TA	1.00E−68
13	Gene 6: Hypothetical protein 3	BGIBMGA000523-TA	1690	10922785	10924187		315	HQ116663	BGIBMGA000523-TA	2.00E−16	BAC Linked to G20, predicted Z-linkage in *O. nubilalis*	66E06, 66M08, 76K21	468	HQ116684	BGIBMGA000523-TA	2.00E−12
14	Gene 4: Cuticular protein	BGIBMGA000520-TA	1690	11249711	11251683	8-09, 8-05	622	HQ116662	BGIBMGA000520-TA	1.00E−23	Z-linked in *O.nubilalis* pedigrees					
15	Gene 3: mRNA binding protein	BGIBMGA000516-TA	1690	11424630	11431079		376	HQ116661	No significant match		Predicted Z-linkage in *O. nubilalis*	76C14, 76G24	361, 329	HQ116683, HQ116682	No significant match	
16	Gene 21: Acyl-CoA dehydrogenase	BGIBMGA000715-TA	1690	11647511	11663115						Predicted Z-linkage in *O. nubilalis*	74K07, 74O15				

Table 5 continued

B. mori chr 1 (Z) gene order	*B. mori/O. nubilalis* Z gene marker	*B. mori* SilkDB Accession #	*B. mori* SilkDB scaffold	*B. mori* position start	*B. mori* position end	*O. nubilalis* polymorphic pedigrees	*O. nubilalis* PCR sequence (bp)	*O. nubilalis* Genbank Accession	*O. nubilalis* SilkDB match	*O. nubilalis* *E* value	*O. nubilalis* current Z Assembly	*O. nubilalis* positive BAC clone	*O. nubilalis* BAC sequence (bp)	*O. nubilalis* Genbank Accession	*O. nubilalis* SilkDB match	*O. nubilalis* *E* value
17	Gene 2: Hypothetical protein 1	BGIBMGA000503-TA	1690	12014499	12023940	8-09, 8-05					Z-linked in *O.nubilalis* pedigrees					
18	Gene 37: ADP-ribosylation factor	BGIBMGA012325-TA	3040	16694222	16701809		275	HQ116681	No significant match		Predicted Z-linkage in *O. nubilalis*					
19	*Gene 38: Amino acid transporter (H-coupled)*	*BGIBMGA012328-TA*	*3040*	*17058197*	*17063187*	*8-05, 8-04*	*592*	HQ116676	*No significant match*		*Paralog amplified, NOT Z-linked in O. nubilalis pedigrees*	*48L17, 48P02*				
20	Gene 32: L-Lactate dehydrogenase	BGIBMGA012336-TA	3040	17340557	17349331	8-09, 8-05, 8-04	468, 489	HQ116679, HQ116680	BGIBMGA012336-TA	1.00E−20	Z-linked in *O.nubilalis* pedigrees	01C10	Coates et al. (2009)			
21	Gene 39: F-box, WD40 domain protein	BGIBMGA012355-TA	3040	18792518	18797632						Predicted Z-linkage in *O. nubilalis*	42G07	622	HQ116691	No significant match	
22	*Gene 33: DNA-binding protein D-ETS-3*	*BGIBMGA012229-TA*	*3040*	*19223701*	*19225441*	*8-09, 8-04*	*480*	HQ116675	*No significant match*		*Paralog amplified, NOT Z-linked in O. nubilalis pedigrees*	*64H03*				
23	Gene 28: Shaker potassium channel	BGIBMGA003851-TA	2734	20911282	20921258	8-05, 8-04	1397	HQ116673	BGIBMGA003851-TA	1.00E−160	Z-linked in *O.nubilalis* pedigrees	75A11				
24	Gene 31: Coatomer protein subunit	BGIBMGA003892-TA	2734	21537446	21554178	8-09, 8-04	587	HQ116674	BGIBMGA003892-TA	5.00E−08	Z-linked in *O.nubilalis* pedigrees	50L01				
25	Gene 30: Leucine zipper transcription factor	BGIBMGA003874-TA	2734	22272508	22280771						Predicted Z-linkage in *O. nubilalis*	53P22				

Roman genes mapped and/or predicted to maintain linkage to the Z chromosome, *italics* gene markers amplifying paralogs (G33 and G38) from another chromosome and predicted translocated genes based on the mapped 8-04 pedigree of marker G23)

Comparative mapping of the Z chromosome

O. nubilalis genetic linkage map assembly

A total of 286, 46, and 134 progeny were genotyped from F_1 pedigrees 8-04, 8-05, and 8-09. Mendelian inheritance of sex linked genes in Lepidoptera predict that an equal proportion of ♂$Z_{A1}Z_{A1}$:♂$Z_{A2}Z_{A1}$:♀ Z_{A1}W:♀ Z_{A2}W genotypes are present among progeny from a cross between a heterozygous (♂$Z_{A1}Z_{A2}$) male and a hemizygous (♀Z_{A1}W) female (Traut and Marec 1997). The Chi-square (χ^2) test statistic indicated significant deviation from predicted 1:1 ratios of hemizygous Z_{A1}W:Z_{A2}W genotypes among F_1 females at markers G23 (pedigree 8-04), G33 (pedigrees 8-04 and 8-09), and G38 (pedigree 8-05, Table 6A) where females displayed an approximate ratio of 1:1 for the Z_{A1}W:$Z_{A1}Z_{A2}$ genotypes. In the pedigree 8-04, the female parent was heterozygous for G23, G33, and G38 suggesting autosomal location (Traut and Marec 1997). Male progeny from pedigrees 8-04, 8-05, and 8-09 deviated significantly from predicted 1:1 $Z_{A1}Z_{A1}$:$Z_{A1}Z_{A2}$ genotypic ratios for marker G23 within pedigree 8-04 (Table 6B), but not at marker loci G33 and G38. The 1:1 Mendelian ratio of $Z_{A1}Z_{A1}$:$Z_{A1}Z_{A2}$ resulted from heterozygous female parents. All other segregating SNP loci appeared to be Z-linked and showed single alleles for female parents as expected for hemizygous WZ individuals. The markers for the *O. nubilalis* genes *ket* (G14) and *ldh* (G32) known to be Z chromosome-linked (Dopman et al. 2005) were inherited in a manner consistent with the anticipated Mendelian genetics for male and female F_1 progeny within all pedigrees that were segregating (Table 6).

Genotype data from the 44 F_1 progeny of pedigree 8-04 were used to determine genetic linkage among SNP- and AFLP-based markers. A total of 139 polymorphic AFLP loci present in the male parent but absent from the female parent were identified, from which χ^2 tests indicated that 101 AFLP loci (72.7%) did not significantly deviate from Mendelian 1:1 genotypic ratios among F_1 progeny ($P \geq 0.05$, data not shown). Genetic linkage was estimated using 28 segregating male progeny from pedigree 8-04 and genotype data from the 101 AFLP and 7 SNP markers that were inherited in a manner consistent with Mendelian segregation. This resulted in 36 predicted linkage groups (LGs, LOD score $\geq$3.0 and recombination fraction $\geq$0.35) with a mean of 3.4 $\pm$ 2.0 markers per linkage group (range 2–10). The number of linkage groups was slightly larger than the known haploid chromosome number ($n = 31$) for *O. nubilalis* (Keil et al. 1990), indicating that an insufficient number of markers were present to construct a complete genetic linkage map. Linkage to the Z chromosome in *O. nubilalis* was detected for 5 AFLP markers (M32, M12, M21, M09, and M36) and the SNP markers G14 (*ket*), G32 (*ldh*), G12, and G31 (Table 7). Of 1.81 million maps generated by bootstrapping, the second most likely map order (presented in Table 7) was chosen over the most likely map order due to its approximate co-linearity with the *B. mori* Z chromosome map (Fig. 1). The order of markers M32 through *ket* showed the second most minimum sum of adjacent recombination fractions (SARF = 0.729) and had an initial map Log-likelihood [Log(L)] of −25.226 compared to the order G31, M32, M12, M21, M09, M36, G32 (*ldh*), G12, and G14 (*ket*) (order 1; SARF = 0.764 and Log(L) = −27.540). The final map spanned 79.3 cM (9.9 $\pm$ 8.4 cM between adjacent markers) with a Log(L) = −2.51. SNP marker data was similarly used to construct separate linkage maps for *O. nubilalis* pedigrees 8-05 and 8-09 (Fig. 1), wherein 7 of 8 and 6 of 8 Z chromosome orthologs showed no significant deviation from predicted Mendelian ratios among female F_1 progeny, respectively (Table 6A). Estimated recombination fractions among male progeny are also shown (Table 6B).

Markers G14 (*ket*), G12, G04, G02, G32 (*ldh*), and G31 were segregating and shown to be linked to the Z chromosome of *O. nubilalis* within at least 2 independent pedigrees (Fig. 1). G13 and G28 (*shkr*) were segregating within pedigree 8-05, and shown to be linked to G14 (*ket*). Additionally, five AFLP-based markers were linked to Z chromosome gene markers in pedigree 8-04. A consensus map of the Z chromosome encompassing a total map distance of 89.0 cM (8.1 $\pm$ 6.2 cM between adjacent markers) was generated using 13 loci (Fig. 1).

Potential O. nubilalis gene rearrangements

Markers for putative Z chromosome orthologs G33 and G38, previously shown to be heterozygous and to significantly deviate from Mendelian-predicted sex-linked genotypic ratios among female progeny in pedigree 8-04 (Table 6A), were not linked to genes known to be on the *O. nubilalis* Z chromosome (*ldh*, *ket*, and *tpi*; Fig. 1; LOD scores = 0 and r.f. $\geq$0.57 compared to markers in Table 7). G33 and G38 were predicted to be linked to a single AFLP marker E-AGC_800M-GAG-0094 (M84), and were within a 13.8 cM region on autosomal LG30. Evidence placing markers G33 (DNA-binding protein D-ETS-3) and G38 (H-coupled amino acid transporter) off of the Z chromosome, and the presence of a heterozygous female parent for these genes confirmed that the genomic position of these two markers was autosomal (Table 6).

Bridging *O. nubilalis* Z chromosome genetic and physical maps

Screening of the *O. nubilalis* BAC library, OnB1, resulted in the identification of at least one clone for 21 of 25

Table 6 Inheritance of Z chromosome linked molecular markers in *O. nubilalis*

Marker locus	*B. mori* ortholog (BGIBMGA)	Pedigree	$Z_{A1}W$	$Z_{A2}W$	$Z_{A1}Z_{A2}$	N	χ^2	*P* value
(A) Test for significant deviation from a Mendelian expected 1:1 ratio of female F_1 hemizygous $Z_{A1}W$ to $Z_{A2}W$ genotypes using Chi-square (χ^2) statistics								
G12	000613-TA	8-04	9	9	0	18	0.000	1.000
G14 (*ket*)	000622-TA	8-04	11	7	0	18	1.000	0.317
G23	001991-TA	8-04	6	1	7	14	7.451	0.006*
G32 (*ldh*)	012336-TA	8-04	9	9	0	18	0.000	1.000
G31	003892-TA	8-04	9	6	0	15	0.063	0.802
G33	012229-TA	8-04	1	5	11	17	7.743	0.006*
G38	012328-TA	8-04	5	3	10	18	1.706	0.192
G02	000503-TA	8-05	61	48	0	109	1.550	0.213
G04	000520-TA	8-05	72	64	0	136	0.471	0.493
G12	000613-TA	8-05	75	68	0	143	0.343	0.558
G13	000619-TA	8-05	75	68	0	143	0.343	0.558
G14 (*ket*)	000622-TA	8-05	69	72	0	141	0.064	0.801
G28 (*shkr*)	003851-TA	8-05	66	73	0	139	0.353	0.553
G32 (*ldh*)	012336-TA	8-05	68	76	0	144	0.444	0.505
G38	012328-TA	8-05	83	0	59	142	<0.001	<0.001*
G02	000503-TA	8-09	30	10	0	40	10.000	0.002*
G04	000520-TA	8-09	33	28	0	61	0.410	0.522
G11	000612-TA	8-09	34	34	0	68	0.001	1.000
G12	000613-TA	8-09	36	31	0	67	0.037	0.541
G13	000619-TA	8-09	37	27	0	64	1.563	0.211
G31	003892-TA	8-09	34	36	0	70	0.057	0.811
G32 (*ldh*)	012336-TA	8-09	32	38	0	70	0.514	0.473
G33	012229-TA	8-09	34	0	26	60	30.533	<0.001*
(B) Test for significant deviation from a Mendelian expected 1:1 ratio of male F1 $Z_{A1}Z_{A1}$ to $Z_{A1}Z_{A2}$ genotypes using Chi-square (χ^2) statistics								
G12	000613-TA	8-04	15	0	13	28	0.143	0.705
G14 (*ket*)	000622-TA	8-04	15	0	11	26	0.615	0.433
G23	001991-TA	8-04	8	8	7	24	4.040	0.044*
G32 (*ldh*)	012336-TA	8-04	15	0	13	28	0.143	0.705
G31	003892-TA	8-04	16	0	10	25	1.385	0.239
G33	012229-TA	8-04	11	0	16	27	0.929	0.335
G38	012328-TA	8-04	8	5	15	28	2.643	0.104
G02	000503-TA	8-05	60	0	44	104	2.462	0.117
G04	000520-TA	8-05	59	0	56	115	0.078	0.780
G12	000613-TA	8-05	63	0	73	136	0.074	0.391
G13	000619-TA	8-05	69	0	64	133	0.188	0.665
G14 (*ket*)	000622-TA	8-05	65	0	71	136	0.265	0.607
G28 (*shkr*)	003851-TA	8-05	70	0	61	131	0.618	0.432
G32 (*ldh*)	012336-TA	8-05	63	0	71	134	0.478	0.490
G38	012328-TA	8-05	66	0	69	135	0.067	0.796
G02	000503-TA	8-09	22	0	28	50	0.720	0.396
G04	000520-TA	8-09	20	0	34	54	3.630	0.057
G11	000612-TA	8-09	39	0	20	59	6.119	0.013*
G12	000613-TA	8-09	35	0	24	59	2.051	0.152
G13	000619-TA	8-09	29	0	28	57	0.018	0.895
G31	003892-TA	8-09	31	0	26	57	0.439	0.508
G32 (*ldh*)	012336-TA	8-09	21	0	35	56	3.500	0.061
G33	012229-TA	8-09	27	0	24	51	0.177	0.674

* Significant deviation with $\alpha < 0.05$

Table 7 Linkage of *O. nubilalis* Z chromosome-like markers in pedigree 8-04

	M32	G31	M09	M36	*ldh*	M21	M12	G12	*ket*
M32	–	0.16	0.24	0.28	0.31	0.18	0.17	0.21	0.26
G31	2.75	–	0.20	0.24	0.24	0.17	0.20	0.21	0.21
M09	1.77	2.09	–	0.03	0.14	0.04	0.07	0.14	0.19
M36	1.31	1.54	6.84	–	0.10	0.07	0.10	0.11	0.15
G32 (*ldh*)	0.93	1.54	3.68	4.54	–	0.11	0.14	0.14	0.19
M21	2.72	2.53	6.56	5.30	4.29	–	0.00	0.07	0.19
M12	2.94	2.09	5.57	4.54	3.68	8.43	–	0.07	0.22
G12	2.11	1.89	3.44	4.29	3.44	5.03	5.30	–	0.12
G14 (*ket*)	1.42	1.89	2.51	3.21	2.51	2.30	1.92	3.79	–

LOD scores and recombination fraction (r.f.) above and below diagonal, respectively

AFLP markers M21 = E-ACC_700M-CAT-0162, M12 = E-AGC_800M-ACG-0176, M09 = E-AGG_800MACG-0285, M36 = E-ACC_700M-ACG-0178, and M32 = E-AGC_800M-TG-0184

orthologs examined (Table 5). Physical linkage was observed for G11 and G12 on BAC clone 64B04, and for G06 and G20 on BAC clone 66E06 (Table 5). The presence of G11 with G12 and G06 with G20 on the same BAC clones agrees with the predicted physical distances of about 14 and 44 kb, respectively, that separate these orthologs on the *B. mori* Z chromosome assembly.

Expression of *O. nubilalis* Z chromosome orthologs

As illustrated in Fig. 2, the overall expression profiles for Z chromosome linked genes in *B. mori* fifth instar tissue samples remained relatively consistent between the two sexes, although many genes had higher apparent dosage in male versus female insects (Zha et al. 2009). While dosage compensation was not analyzed in *O. nubilalis* expression profiles, a visual comparative assessment of gene expression profiles for mapped or predicted Z-linked genes indicated similar expression patterns for approximately 75% of the *O. nubilalis* orthologs when compared to the *B. mori* fifth instar larval tissue microarray data (Fig. 2). The presence or absence of transcripts was analyzed for 38 Z chromosome orthologs across *O. nubilalis* growth stages and tissues (Fig. 2), for which constitutive expression of a single RT-PCR product across all tissues and life stages was shown for 15 genes: G03, G10, G13, G14 (*ket*), G15, G16, G17, G20, G23, G27, G28 (*shkr*), G29, G31, G37, G43 (*tpi*). In contrast, transcripts detected for orthologs G04, G05, G06, G08, G11, G12, G22, G26, G34, G36, G40, and G39 showed differential expression across growth stages or tissues, of which G22 and G26 appeared to be preferentially expressed in the adult male (Fig. 2). Expression profiles for G04, G05, G26, G36, and G42 were consistent among replicates, but showed some unexpected trends when comparing the fourth and fifth instars. Transcripts for those genes were detected in certain tissues from the fourth and fifth instars, but were below the limits of detection in whole larvae (see "Discussion" for further comments). Loci near G04 also showed relatively low expression in *B. mori* fifth instar larval tissues, and this is consistent with the limited expression observed in *O. nubilalis* fifth instar tissues. Profiles for G06, G08, G09, G12, G15, G18, G19, G21, G24, G25, G26, G30 G32 (*ldh*), G34, G36, G39, G40, G41, and G42 displayed multiple bands indicating the possibility of alternative splice variants for these orthologs in the cDNA pools that were tested (Fig. 2). G25 also showed expression of large transcripts specific to

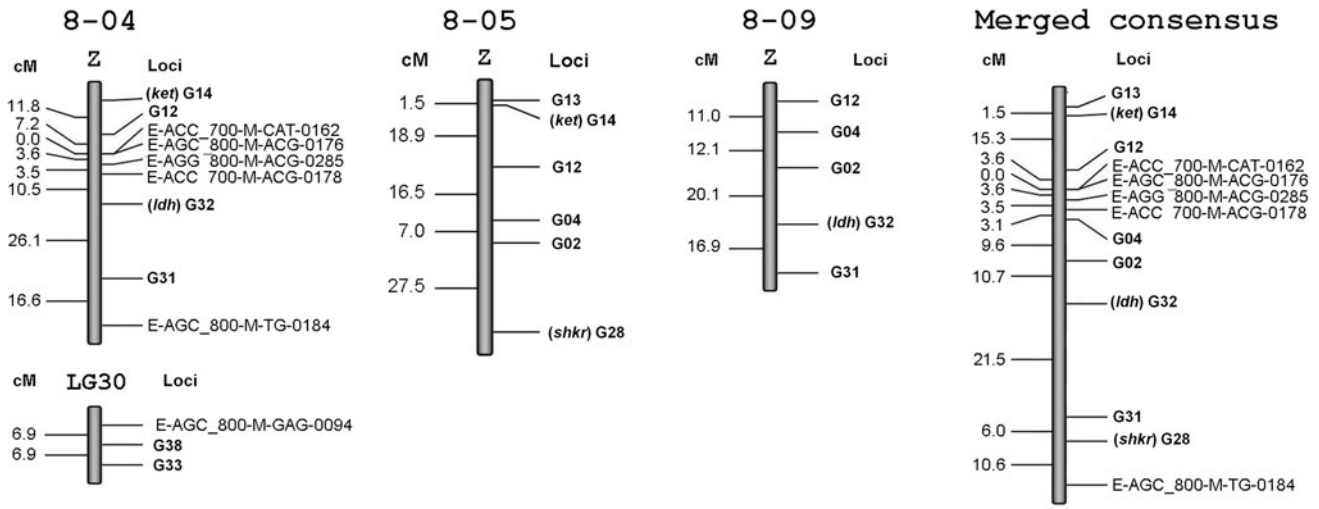

Fig. 1 Predicted linear order and centi-Morgan (cM) distances between *O. nubilalis* markers developed from orthologs on the *B. mori* Z chromosome. LG30 represents a possible translocation of markers 33 and 38 to an autosomal locus that co-segregates with an AFLP in the 8-04 pedigree and which is syntenic to a region on *B. mori* Chromosome 13

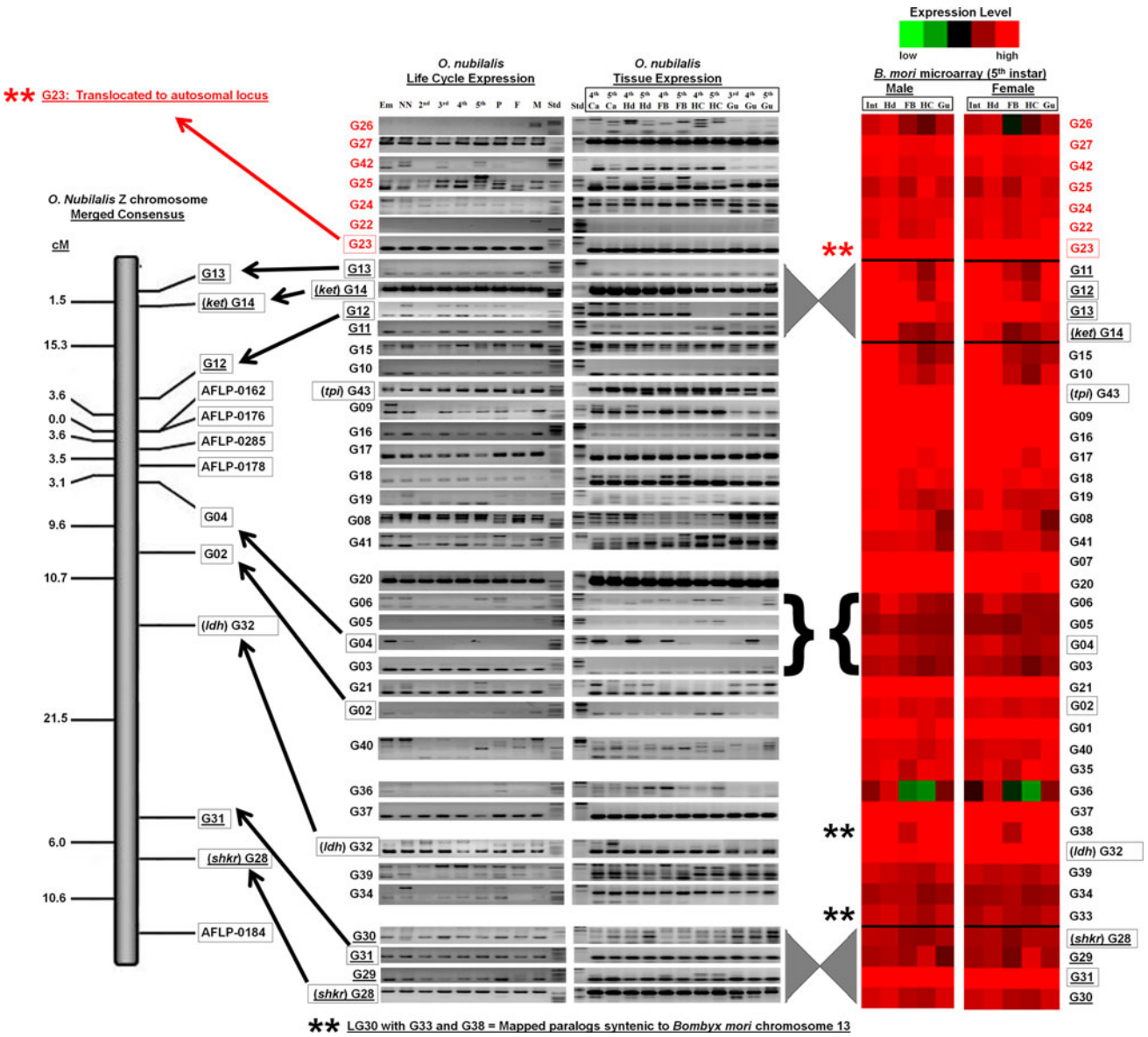

Fig. 2 Expression profiling of *O. nubilalis* genes compared to the microarray expression data of Z-linked gene orthologs in tissues of fifth instar *B. mori* larvae. Constitutive, tissue-specific, and life-stage specific profiles exist for Z gene orthologs in *O. nubilalis*. Although not shown, banding patterns are representative of all three biological expression replicates gathered for each individual gene. Expression profiles varied for tissues between *O. nubilalis* and *B. mori*, although qualitative assessment of the data indicate relative conservation in patterns for many genes in the fifth instar tissues. This is most clear for the homologs G03–G06 that showed lower levels of expression in *B. mori* and were near the limits of detection in *O. nubilalis* (*indicated by braces*). Splice variants are apparent in the cDNA expression profiles for 18 genes (G06, G08, G09, G12, G18, G19, G21, G24, G25, G26, G30, G32 (*ldh*), G34, G36, G39, G40, G41, and G42) analyzed in *O. nubilalis*. Inversions are apparent at both *O. nubilalis* Z chromosome ends (*crosses*) compared to the *B. mori* chromosome 1 scaffold. These are associated with changes in gene expression. This is clear for G28 expression, which is robust in *O. nubilalis*, but is expected be near the limits of detection (like G04) based on the relatively low expression levels observed in *B. mori*. A putative autosomal translocation of G23 off the Z chromosome in *O. nubilalis* (*asterisks, top*) was identified by mapping. Autosomal genes were detected that are likely to be paralogs of G33 and G38 (*asterisks, bottom*). Em, embryo; NN, neonate; second–fifth, larval instars; *P* pupae, *F* female adult, *M* male adult, *Ca* carcass, *Hd* head, *FB* fat body, *HC* hemocytes, *Gu* gut, *Int* integument, *Std* molecular standards. *B. mori* raw microarray data was retrieved and analyzed from SilkDB (Duan et al. 2010; Xia et al. 2007; Zha et al. 2009). Loci that mapped to the *O. nubilalis* Z chromosome are *boxed*. Except for identified inversions, the genes are presented in the order in which they appear on the *B. mori* Z chromosome and chromosome 13. Primer pairs for G01, G07 and G35 were located immediately adjacent to and across large intronic sequences, and failed to amplify PCR products from *O. nubilalis* cDNA

fifth instar Ca, Hd, and FB tissue samples (Fig. 2). Unexpected patterns were observed for loci at the end of the Z chromosome where linkage mapping indicated there is an inversion in *O. nubilalis* relative to *B. mori*. In *B. mori*, expression levels for loci near G28 (*shkr*) display lower levels of expression in the fifth instar tissues. While these loci would be expected to be near the limits of detection (based on our observations of loci in the G04 region), RT-PCR products were relatively intense. These patterns were consistent across replicates.

Discussion

Genes encoded on the Z chromosome of Lepidoptera are involved in the differentiation of ecotypes and speciation (Hagen and Scriber 1989; Sperling 1994; Jiggins et al. 2001a, b), but the isolation of genes or chromosome regions regulating these traits is hindered in part by the absence of a dense genetic linkage map for each species (Marcus 2005). To partially address these shortfalls, we created a genetic linkage map for the *O. nubilalis* Z chromosome that was based on gene orthologs that can be identified across multiple species of Lepidoptera. The *O. nubilalis* map is one of the most comprehensive reported to date for a Z chromosome in Lepidoptera with a total of 13 markers that span 89.0 cM (8.1 ± 6.2 cM between markers). Intervals on the *O. nubilalis* Z chromosome that influence diapause (*pdd*) and pheromone response (*resp*) QTL have been identified, where a *tpi* polymorphism shows tight linkage with *pdd* (Glover et al. 1992; Dopman et al. 2004, 2005). A BAC clone encompassing the *tpi* locus was identified and will be a valuable resource for isolating the putative genome region encompassing *pdd* (Coates et al. 2009). Dopman et al. (2005) positioned the *resp* QTL 20.0 cM from *ldh* and ~7.5 cM from the microsatellite marker ma169. The merged map generated in this study placed markers G31 and G28 (*shkr*) in the vicinity of the predicted *resp* QTL, and are ~21.5 and 27.5 cM from *ldh*, respectively. Estimates from *B. mori* suggest there are about 0.25 Mbp of physical distance per cM (Xiang et al. 2008), but this estimate may vary across genome intervals and species due to chromosomal structural differences (Roberts 1965; Myers et al. 2005). If a similar physical distance per cM exists in *O. nubilalis,* markers G31 and G28 could be located within 0.375 to 1.875 Mb of *resp*, a distance that could likely be easily spanned using BAC clones from the OnB1 library.

In addition to being a genomic resource for *O. nubilalis*, the orthologous SNP markers for the Z chromosome will be a useful tool for comparative analysis among species of Lepidoptera, as we predicted orthology for 43 loci from 10 species by PCR screening (Table 4). Putatively orthologous markers need to be further validated as true orthologs by sequencing and database comparisons if legitimate conclusions regarding structural genome evolution are to be drawn from resulting datasets (Devos et al. 1999; Doganlar et al. 2002). Sequencing and evidence of map position were used to further validate orthology among the 13 markers co-segregating on the *O. nubilalis* Z chromosome, which suggested that 3 homologous loci (G23, G33, and G38) in *O. nubilalis* did not co-segregate with the known Z chromosome anchor markers, G14 (*ket*) and G32 (*ldh*) (Table 6).

Aberrations involving breakage, fusion, inversion and translocation of chromosomal regions occur throughout evolution, and the resulting rearrangements often define differences between closely related species (Kirkpatrick and Barton 2006). Chromosomal mutations are not uncommon in the Lepidoptera (Marec et al. 2001; Rego and Marec 2003; Sahara et al. 2003; Yokoyama et al. 2003; Abe et al. 2005), and have even been used to facilitate fine mapping of Z chromosome regions in *B. mori* (Fujii et al. 2008). Using three aberrant chromosomes resulting from intra and inter-chromosomal recombination, Fujii et al. (2008) fine mapped the chromosome breakage points and isolated a candidate gene for the distinct oily (*od*) mutant phenotype in the silkworm. A translocation event between the W and Z chromosomes was documented to result in a hybrid WZ chromosome causing a lethal phenotype when transmitted to female progeny (Fujii et al. 2006). Additional rearrangements have been documented to cause male muscle dystrophy and abnormal oogenesis in *B. mori* females (Fujii and Shimada 2007).

Translocations of a Z chromosome region carrying sex-linked recessive lethal mutations have been used to create balanced lethal strains in *B. mori* (Strunnikov 1975) and the Mediterranean flour moth, *Ephestia kuehniella* (Marec 1990), but were induced through the use of mutagens (North and Holt 1968). Naturally occurring chromosomal breakage and fusions have been reported in the Sonoran blue butterfly, *Philotes sonorensis* (Emmel et al. 1973), that may be involved in the evolution of the supernumerary A and B chromosomes (Maeki 1958). We provided evidence that three putative Z chromosome orthologs are inherited as autosomal loci (G23, G33, and G38), which suggests that these markers could each be detecting a paralogous gene or a genome rearrangement compared to *B. mori*. The two putative chromosome rearrangements are addressed below.

The first putative translocation involves marker G23 that showed autosomal inheritance in *O. nubilalis*. G23 is a homolog of the ribosomal protein L36E gene (rpL36E) that is located at nucleotide positions 4,988,669–4,991,978 on *B. mori* chromosome 1. Sequencing confirmed that G23 shares 65% identity and 80% homology to amino acids encoded by nucleotide positions 37–126 of the *B. mori*

rpL36E gene (BGIBMGA001991). Although our tblastx search of the *B. mori* genome sequence indicated that closely related paralogs are not present within the assembly (*E*-values $\leq$ 3.2), we cannot exclude the possibility that marker G23 may be detecting a paralog within the *O. nubilalis* genome. It is also possible that the ortholog of the rpL36E gene does exist on the *O. nubilalis* Z chromosome, but that it failed to be amplified by our degenerate primers. The mapping of markers that flank G23 may provide confirmatory evidence for this putative translocation, and this is being pursued.

The second putative translocation involved two markers, G33 and G38, which co-segregated with one another and a single AFLP marker. Since the orthologous *B. mori* Z chromosome region between the G33 and G38 homologs (positions 17,058,197–19,225,441) includes the *ldh* gene (positions 17,340,557–17,349,331), retention of the *ldh* marker on the *O. nubilalis* Z chromosome would necessitate changes in micro-synteny prior to the translocation. Investigation of the *B. mori* genome assembly indicated that chromosome 13 contained potential paralogs for both G33 and G38. Specious detection of gene BGIBMGA001167 on chromosome 13 by primers targeting G33 (BGIBMGA012229) may be due to both genes being annotated as DNA-binding ETS-domain containing transcription factors. Analogously, the *B. mori* Z chromosome-linked homolog of G38 (BGIBMGA012328) shows high levels of homology with BGIBMGA001299 on chromosome 13, thus these two annotated amino acid transporter genes likely represent paralogs within the *B. mori* genome. Although not intended, the present study indicates that these orthologous regions of the *B. mori* chromosome 13 are conserved in *O. nubilalis*. It is possible that homologs of these genes also exist on the *O. nubilalis* Z chromosome, but failed to be isolated using our current methods. While G33 and G38 failed to contribute to our analysis of the *O. nubilalis* Z chromosome, the autosomal mapping of these loci highlights the need for scrutiny during marker validation to avoid spurious detection of structural changes between species (Fulton et al. 2002).

The comparison of synteny and co-linearity among genomes has been shown to be an effective method to identify ancestral linkage relationships and genome-level rearrangements (Feltus et al. 2006; Fredslund et al. 2006) and also to map shared traits (Schmidt 2000; Delseny 2004). Compared to *B. mori*, markers for the genes *tpi* and *apterous* were shared on the Z chromosome of the postman butterfly *H. melpomene* (Yasukochi et al. 2006) and inversions have been demonstrated in the squinting bush brown butterfly *Bicyclus anynana* (Beldade et al. 2009). Compared to the *B. mori* chromosome 1 (Z), the *B. anynana* inversions took place in regions syntenic to positions 1–10.88 Mb, but as Lepidoptera have holocentric chromosomes that do not exhibit primary constrictions indicative of centromeres (Murakami and Imai 1974), we cannot assign such rearrangements to chromosome "arms" (Wolf 1996). The tobacco hornworm moth *Manduca sexta* was found to have an inversion (relative to *B. mori*) encompassing nearly half of the Z chromosome (Yasukochi et al. 2009), and studies by Beldade et al. (2009) and Yasukochi et al. (2009) confirm that rearrangements have affected the structures of the Z chromosome among lepidopteran lineages. Compared to the *B. mori* physical map, the *O. nubilalis* genetic linkage map predicted two putative inversions, one involving markers G31 and G28, and the second involving markers G12, G13, and G14 (Figs. 1, 2).

The first putative inversion involved markers G31 and G28 in *O. nubilalis* and is similar to the Z chromosome inversion present in *M. sexta* (Yasukochi et al. 2009). Although speculative in lieu of analogous genetic linkage map data from other species and additional flanking orthologous markers in *O. nubilalis*, inversions in this region may be a common feature of the Z chromosome in moths when compared to butterfly lineages.

The second putative inversion involves a 16.8 cM region of the *O. nubilalis* Z chromosome defined by markers G12, G13, and G14. The structural change involved a large segment that was also shown to be inverted in *B. anynana* (Beldade et al. 2009), and indicates the inversion may be common across multiple lineages of Lepidoptera. Despite confidence in the detection of this gross structural change, the juxtaposition of closely spaced markers G13 and G14 complicates the accuracy of predicted rearrangements and fine-scale inversions may be present. Given the proximity of orthologous markers G13 and G14 in the *B. mori* genome ($\sim$0.5 Mb apart), data from our F_1 progeny are not sufficient for fine mapping. In order to provide higher resolution and the ability to estimate micro-synteny, a larger number of recombinants is typically required (Darvasi and Soller 1995). Some degree of shared micro-synteny was identified in our study by the isolation of a single OnB1 BAC clone (64B04) that contains the orthologs G11 and G12 which, in the *B. mori* genome, are spaced within a 14.6 kb interval.

Expression of *O. nubilalis* Z chromosome orthologs

Synteny and conservation of gene orders on the Z chromosome among lepidopteran lineages predicts that some level of conservation for gene expression patterns could also exist between species. Although dosage compensation could not be assessed by our RT-PCR analyses that were more qualitative than quantitative, the tissue-specific expression profiles for Z chromosome gene orthologs in *O. nubilalis* were qualitatively similar to expression levels found in fifth instar *B. mori* larvae (Fig. 2). This is

exemplified by the region encompassing markers G03–G06 where expression was difficult to detect in *O. nubialis* fifth instar tissues and also shows reduced expression levels in *B. mori* fifth instar tissues (Fig. 2). On the other hand, robust detection of transcripts near the end of the Z chromosome was unexpected as was the case for G28 (*shkr*), and demonstrates that a chromosomal rearrangement may be associated with altered transcript levels of this gene in *O. nubilalis* compared to *B. mori.*

The region of the Z chromosome spanning G04–G06 in *O. nubilalis* also showed consistent transcriptional regulation (G06 and G05 with preference for HC expression; G04 encoding a cuticular protein transcript observed specifically in NN larvae and premolt fourth instar Ca, Hd, FB, and Gu tissue samples), suggesting that regulated transcriptional controls have evolved for these genes in *O. nubilalis*. Additionally, G25 also displayed a large transcript splice variant only apparent in the fifth instar Ca, Hd, and FB samples (Fig. 2). Specific expression in FB and HC samples may be indicative of transcripts involved in regulating immune functions, whereas the tight regulation of the mapped cuticular protein gene G04 may be due to specific restructuring events targeted during molts. Gene induction and silencing for specific temporal events during immune cascades, metamorphosis, starvation, and environmental responses is common and has been demonstrated with many lepidopteran microarrays and EST profiles (Halitschke et al. 2003; Davies et al. 2006; Cheng et al. 2008; Khajuria et al. 2009).

The expression patterns for G04, G05, G26, G36, and G42, showed consistent expression in tissue replicates from fourth instars but did not appear in the fourth instar whole larval samples from life-cycle replicates. The amount of tissue-specific material used for template cDNA production in pooled tissue samples (10–40 individuals) was well over an order of magnitude greater than what would have been represented by the one or two fourth and fifth instar larvae used in the whole body life cycle samples (see "Materials and methods"). Thus, weakly expressed gene transcripts may be below detection levels in life cycle screens but show up strongly in pooled tissue samples from 10 to 50 representative larvae.

Comparative analyses of gene expression between *B. mori* and *O. nubilalis* were further complicated by what appear to be splice variants for markers G06, G08, G09, G12, G18, G19, G21, G24, G25, G26, G30, G32 (*ldh*), G34, G36, G39, G40, G41, and G42, where these alternative splice variations would not be accounted for in the analysis of *B. mori* microarray data (Fig. 2). Alternatively, the observed cDNA profiles may result from the concurrent PCR amplification of multiple paralogs. Extended analyses to resolve the gene sequence of alternative transcripts for life-stage specific, tissue specific, and genes exhibiting multiple PCR bands in expression profiles are currently underway.

Further assessment will be required to elucidate the factors regulating genes present on the *O. nubilalis* Z chromosome. Nevertheless, these data offer interesting insights and generalizations regarding the expression of Z-linked genes in Lepidoptera, and open new possibilities for comparative genomic evaluation between species.

Conclusions

Increased resolution of the *O. nubilalis* Z chromosome map will provide a platform for future mapping of additional sex-linked traits and for identifying the QTL governing pheromone induced male behavior and voltinism in this insect. These traits can be extremely important for all pest species whose inherent ability to find mates and whose generation times directly impact the establishment of economic injury levels in agricultural systems. This study provides an enhanced map of the Z chromosome in *O. nubilalis*, incorporating and comparing a genetic map, gene expression data, and sequence data gathered for a panel of 43 genes that, based on the *B. mori* genome assembly, were predicted to be sex-linked in *O. nubilalis*. These results suggest the existence of chromosomal rearrangements occurring in *O. nubilalis* compared to *B. mori* and also provide a solid platform for analyzing and genotyping sex-linked traits in pest populations. The expression data described by this study offer a novel glimpse into the life-stage and tissue-specific expression for sex-linked genes in *O. nubilalis*, allowing for new predictions in gene activity to be made for this agriculturally relevant insect. The data presented herein also provide new and valuable insights into the evolution of lepidopteran chromosomal structures.

Acknowledgments This research was a joint contribution from the USDA, Agricultural Research Service and the Iowa Agriculture and Home Economics Experiment Station, Ames, IA (project 3543), and was supported by USDA-ARS-CRIS-017. This article reports the results of research only. Mention of a proprietary product does not constitute an endorsement or a recommendation by USDA or Iowa State University for its use. The authors would like to thank Mike Rausch and Elizabeth Schrum for their contributions to BAC sequencing of OnB1 Z chromosome clones.

References

Abe H, Seki M, Ohbayashi F, Tanaka N, Yamashita J, Fujii T, Yokoyama T, Takahashi M, Banno Y, Sahara K, Yoshido A, Ihara J, Yasukochi Y, Mita K, Ajimura M, Suzuki MG, Oshiki T, Shimada T (2005) Partial deletions of the W chromosome due to reciprocal translocation in the silkworm *Bombyx mori*. Insect Mol Biol 14:339–352

Altermatt F (2010) Climatic warming increases voltinism in European butterflies and moths. Proc Biol Sci 277:1281–1287

Arbuthnot KD (1949) Temperature and precipitation in relation to the number of generations of European corn borer in the United States. USDA Tech Bull 987

Beldade P, Saenko SV, Pul N, Long AD (2009) A gene-based linkage map for *Bicyclus anynana* butterflies allows for a comprehensive analysis of synteny with the Lepidopteran reference genome. PLoS Genet 5:e1000366

Cheng TC, Zhang YL, Liu C, Xu PZ, Gao ZH, Xia QY, Xiang ZH (2008) Identification and analysis of Toll-related genes in the domesticated silkworm, *Bombyx mori*. Dev Comp Immunol 32:464–475

Coates BS, Hellmich RL (2003) Two sex-chromosome-linked microsatellite loci show geographic variance among North American *Ostrinia nubilalis*. J Insect Sci 3:29

Coates BS, Sumerford DV, Hellmich RL, Lewis LC (2007) A beta-1,3-galactosyltransferase and brainiac/bre5 homolog expressed in the midgut did not contribute to a Cry1Ab toxin resistance trait in *Ostrinia nubilalis*. Insect Biochem Mol Biol 37:346–355

Coates BS, Sumerford DV, Hellmich RL, Lewis LC (2008) Mining an *Ostrinia nubilalis* midgut expressed sequence tag (EST) library for candidate genes and single nucleotide polymorphisms (SNPs). Insect Mol Biol 17:607–620

Coates BS, Sumerford DV, Hellmich RL, Lewis LC (2009) Repetitive genome elements in a European corn borer, *Ostrinia nubilalis*, bacterial artificial chromosome library were indicated by bacterial artificial chromosome end sequencing and development of sequence tag site markers: implications for lepidopteran genomic research. Genome 52:57–67

Coates BS, Sumerford DV, Hellmich RL, Lewis LC (2010) A helitron-like transposon superfamily from lepidoptera disrupts (GAAA)(*n*) microsatellites and is responsible for flanking sequence similarity within a microsatellite family. J Mol Evol 70:275–288

Darvasi A, Soller M (1995) Advanced intercross lines, an experimental population for fine genetic mapping. Genetics 141:1199–1207

Davies L, Williams DR, Aguiar-Santana IA, Pedersen J, Turner PC, Rees HH (2006) Expression and down-regulation of cytochrome P450 genes of the CYP4 family by ecdysteroid agonists in *Spodoptera littoralis* and *Drosophila melanogaster*. Insect Biochem Mol Biol 36:801–807

de Hoon MJ, Imoto S, Nolan J, Miyano S (2004) Open source clustering software. Bioinformatics 20:1453–1454

Delseny M (2004) Re-evaluating the relevance of ancestral shared synteny as a tool for crop improvement. Curr Opin Plant Biol 7:126–131

Devos KM, Beales J, Nagamura Y, Sasaki T (1999) Arabidopsis-rice: will colinearity allow gene prediction across the eudicot–monocot divide? Genome Res 9:825–829

Doganlar S, Frary A, Daunay M-C, Lester RN, Tanksley SD (2002) A comparative genetic linkage map of eggplant (*Solanum melongena*) and its implications for genome evolution in the Solanaceae. Genetics 161:1697–1711

Dopman EB, Bogdanowicz SM, Harrison RG (2004) Genetic mapping of sexual isolation between E and Z pheromone strains of the european corn Borer (*Ostrinia nubilalis*). Genetics 167:301–309

Dopman EB, Perez L, Bogdanowicz SM, Harrison RG (2005) Consequences of reproductive barriers for genealogical discordance in the European corn borer. Proc Natl Acad Sci USA 102:14706–14711

Dopman EB, Robbins PS, Seaman A (2010) Components of reproductive isolation between North American pheromone strains of the European corn borer. Evolution 64:881–902

Duan J, Li R, Cheng D, Fan W, Zha X, Cheng T, Wu Y, Wang J, Mita K, Xiang Z, Xia Q (2010) SilkDB v2.0: a platform for silkworm (*Bombyx mori*) genome biology. Nucleic Acids Res 38:D453–D456

Emmel TC, Trew HR, Shields O (1973) Chromosomal variability in a Nearctic lycaenid butterfly, *Philotes sonorenis* (Lepidoptera: Lycaenidae). Pan Pacific Entomol 49:74–80

Falk CT (1992) Preliminary ordering of multiple linked loci using pairwise linkage data. Genet Epidemiol 9:367–375

Feltus FA, Singh HP, Lohithaswa HC, Schulze SR, Silva T, Paterson AH (2006) Conserved intron scanning primers: targeted sampling of orthologous DNA sequence diversity in orphan crops. Plant Physiol 140:1183–1191

Ferveur J-F, Stortkuhl KF, Stocker RF, Greenspan RJ (1995) Genetic feminization of brain structures and changed sexual orientation in male *Drosophila*. Science 267:902–905

Fredslund J, Madsen LH, Hougaard BK, Nielsen AM, Bertioli D, Sandal N, Stougaard J, Schauser L (2006) A general pipeline for the development of anchor markers for comparative genomics in plants. BMC Genomics 7:207

Fujii T, Shimada T (2007) Sex determination in the silkworm, *Bombyx mori*: a female determinant on the W chromosome and the sex-determining gene cascade. Semin Cell Dev Biol 18:379–388

Fujii T, Tanaka N, Yokoyama T, Ninaki O, Oshiki T, Ohnuma A, Tazima Y, Banno Y, Ajimura M, Mita K, Seki M, Ohbayashi F, Shimada T, Abe H (2006) The female-killing chromosome of the silkworm, *Bombyx mori*, was generated by translocation between the Z and W chromosomes. Genetica 127:253–265

Fujii T, Abe H, Katsuma S, Mita K, Shimada T (2008) Mapping of sex-linked genes onto the genome sequence using various aberrations of the Z chromosome in *Bombyx mori*. Insect Biochem Mol Biol 38:1072–1079

Fulton TM, Van der Hoeven R, Eannetta NT, Tanksley SD (2002) Identification, analysis, and utilization of conserved ortholog set markers for comparative genomics in higher plants. Plant Cell 14:1457–1467

Glover TJ, Tang X-H, Roelofs WL (1987) Sex pheromone blend discrimination by male moths from E and Z strains of European corn borer. J Chem Ecol 13:143–151

Glover TJ, Robbins PS, Eckenrode CJ, Roelofs WL (1992) Genetic control of voltinism characteristics in European corn borer races assessed with a gene marker. Arch Insect Biochem Physiol 20:107–117

Gotter AL, Levine JD, Reppert SM (1999) Sex-linked period genes in the silkmoth, *Antheraea pernyi*: implications for circadian clock regulation and the evolution of sex chromosomes. Neuron 24:953–965

Gould F, Estock M, Hillier NK, Powell B, Groot AT, Ward CM, Emerson JL, Schal C, Vickers NJ (2010) Sexual isolation of male moths explained by a single pheromone response QTL containing four receptor genes. Proc Natl Acad Sci USA 107:8660–8665

Guthrie WD (1990) Advances in rearing the European corn borer on ameridic diet. In: Proceedings, international symposium on methodologies for developing resistance to insects. CIMMYT (International Maize and Wheat Improvement Center) Texcoco, Mexico

Hagen RH, Scriber JM (1989) Sex-linked diapause, color, and allozyme loci in *Papilio glaucus*: linkage analysis and significance in a hybrid zone. Heredity 80:179–185

Hairston NG Jr, Kearns CM (1995) The interaction of photoperiod and temperature in diapause timing: a copepod example. Biol Bull 189:42–48

Halitschke R, Gase K, Hui D, Schmidt DD, Baldwin IT (2003) Molecular interactions between the specialist herbivore

Manduca sexta (Lepidoptera, Sphingidae) and its natural host *Nicotiana attenuata*. VI. Microarray analysis reveals that most herbivore-specific transcriptional changes are mediated by fatty acid-amino acid conjugates. Plant Physiol 131:1894–1902

Hall TA (1999) BioEdit: a user-friendly biological sequence alignment editor and analysis program for Windows 95/98/NT. Nucleic Acids Symp Ser 41:95–98

Hunter MD, McNeil JN (1997) Host-plant quality influences diapause and voltinism in a polyphagous insect herbivore. Ecology 78:977–986

Jiggins CD, Linares M, Naisbit RE, Salazar C, Yang ZH, Mallet J (2001a) Sex-linked hybrid sterility in a butterfly. Evolution 55:1631–1638

Jiggins CD, Naisbit RE, Coe RL, Mallet J (2001b) Reproductive isolation caused by colour pattern mimicry. Nature 411:302–305

Kanzaki R, Soo K, Seki Y, Wada S (2003) Projections to higher olfactory centers from subdivisions of the antennal lobe macroglomerular complex of the male silkmoth. Chem Senses 28:113–130

Karpati Z, Dekker T, Hansson BS (2008) Reversed functional topology in the antennal lobe of the male European corn borer. J Exp Biol 211:2841–2848

Keil CB, Mason CE, Showers WB (1990) Apyrene spermatogenesis in *Ostrinia nubilalis* (Hubner): obligate and facultative diapausing strains. J Hered 81:72–74

Khajuria C, Zhu YC, Chen MS, Buschman LL, Higgins RA, Yao J, Crespo AL, Siegfried BD, Muthukrishnan S, Zhu KY (2009) Expressed sequence tags from larval gut of the European corn borer (*Ostrinia nubilalis*): exploring candidate genes potentially involved in *Bacillus thuringiensis* toxicity and resistance. BMC Genomics 10:286

Kirkpatrick M, Barton N (2006) Chromosome inversions, local adaptation and speciation. Genetics 173:419–434

Klun JA (1975) Insect sex pheromones: intraspecific pheromonal variability of *Ostrinia nubilalis* in North America and Europe. Environ Entomol 4:891–894

Lassance JM, Groot AT, Lienard MA, Antony B, Borgwardt C, Andersson F, Hedenstrom E, Heckel DG, Lofstedt C (2011) Allelic variation in a fatty-acyl reductase gene causes divergence in moth sex pheromones. Nature 466:486–489

Lincoln SD, Daly M, Lander ES (1992) Constructing genetic maps with MAPMAKER/EXP 3.0. Whitehead Institute Technical Report, 3rd edn

Liu Z, Gong P, Li D, Wei W (2010) Pupal diapause of *Helicoverpa armigera* (Hubner) (Lepidoptera: Noctuidae) mediated by larval host plants: pupal weight is important. J Insect Physiol 56:1863–1870

Lofstedt C, Hansson BS, Roelofs W, Bengtsson BO (1989) No linkage between genes controlling female pheromone production and male pheromone response in the European corn borer, *Ostrinia nubilalis* Hubner (Lepidoptera; Pyralidae). Genetics 123:553–556

Maeki K (1958) On the chromosomes of *Pieris rapae* (Lepidoptera: Rhopalocera). Jpn J Genet 33:398–404

Marcus JM (2005) Jumping genes and AFLP maps: transforming lepidopteran color pattern genetics. Evol Dev 7:108–114

Marec F (1990) Genetic control of pest Lepidoptera: induction of sex-linked recessive lethal mutations in *Ephestia kuehniella* (Pyralidae). Acta Entomol Bohemoslov 87:445–458

Marec F, Tothova A, Sahara K, Traut W (2001) Meiotic pairing of sex chromosome fragments and its relation to atypical transmission of a sex-linked marker in *Ephestia kuehniella* (Insecta: Lepidoptera). Heredity 87:659–671

McLeod DGR (1976) Geographical variation of diapause termination in the European corn borer, *Ostrinia nubilalis* (Lepidoptera: Pyralidae) in southwestern Ontario. Can Entomol 108:1403–1407

Miao XX, Li WH, Li MW, Zhao YP, Guo XR, Huang YP (2008) Inheritance and linkage analysis of co-dominant SSR markers on the Z chromosome of the silkworm (*Bombyx mori* L.). Genet Res 90:151–156

Murakami A, Imai HT (1974) Cytological evidence for holocentric chromosomes of the silkworms, *Bombyx mori* and *B. mandarina*, (Bombycidae, Lepidoptera). Chromosoma 47:167–178

Myers S, Bottolo L, Freeman C, McVean G, Donnelly P (2005) A fine-scale map of recombination rates and hotspots across the human genome. Science 310:321–324

Nagaraja GM, Mahesh G, Satish V, Madhu M, Muthulakshmi M, Nagaraju J (2005) Genetic mapping of Z chromosome and identification of W chromosome-specific markers in the silkworm, *Bombyx mori*. Heredity 95:148–157

North DT, Holt OO (1968) Inherited sterility in progeny of irradiated male cabbage loopers. J Econ Entomol 61:928–931

Olsson SB, Kesevan S, Groot AT, Dekker T, Heckel DG, Hansson BS (2010) *Ostrinia* revisited: Evidence for sex linkage in European Corn Borer *Ostrinia nubilalis* (Hubner) pheromone reception. BMC Evol Biol 10:285

Palli SR, Ladd TR, Ricci AR, Primavera M, Mungrue IN, Pang AS, Retnakaran A (1998) Synthesis of the same two proteins prior to larval diapause and pupation in the spruce budworm, *Choristoneura fumiferana*. J Insect Physiol 44:509–524

Pringle EG, Baxter SW, Webster CL, Papanicolaou A, Lee SF, Jiggins CD (2007) Synteny and chromosome evolution in the Lepidoptera: evidence from mapping in *Heliconius melpomene*. Genetics 177:417–426

Rego A, Marec F (2003) Telomeric and interstitial telomeric sequences in holokinetic chromosomes of Lepidoptera: telomeric DNA mediates association between postpachytene bivalents in achiasmatic meiosis of females. Chromosome Res 11:681–694

Roberts PA (1965) Difference in the behavior of eu- and heterochromatin: crossing-over. Nature 205:725–726

Roelofs W, Glover T, Tang XH, Sreng I, Robbins P, Eckenrode C, Lofstedt C, Hansson BS, Bengtsson BO (1987) Sex pheromone production and perception in European corn borer moths is determined by both autosomal and sex-linked genes. Proc Natl Acad Sci USA 84:7585–7589

Rozen S, Skaletsky HJ (2000) Primer3 on the WWW for general users and for biologist programmers. In: Krawetz S, Misener S (eds) Bioinformatics methods and protocols: methods in molecular biology. Humana Press, Totowa, NJ, pp 365–386

Sahara K, Yoshido A, Kawamura N, Ohnuma A, Abe H, Mita K, Oshiki T, Shimada T, Asano S, Bando H, Yasukochi Y (2003) W-derived BAC probes as a new tool for identification of the W chromosome and its aberrations in *Bombyx mori*. Chromosoma 112:48–55

Saldanha AJ (2004) Java Treeview—extensible visualization of microarray data. Bioinformatics 20:3246–3248

Schmidt R (2000) Synteny: recent advances and future prospects. Curr Opin Plant Biol 3:97–102

Showers WB (1979) Effects of diapause on the migration of the European corn borer into the southeastern United States. In: Rabb RL, Kennedy GG (eds) Movement of highly mobile insects: concepts and methodology in research. North Carolina St. University Press, pp 420–430

Showers WB, Brindley TA, Reed GL (1972) Survival and diapause characteristics of hybrids of three geographical races of the European corn borer. Ann Entomol Soc Am 65:450–457

Showers WB, Chiang HC, Keaster AJ, Hill RE, Reed GL, Sparks AN, Musick GJ (1975) Ecotypes of the European corn borer in North America. Environ Entomol 4:753–760

Sperling FAH (1994) Sex-linked genes and species differences in Lepidoptera. Can Entomol 126:807–818

Strunnikov VA (1975) Sex control in silkworms. Nature (Lond.) 255:111–113

Tamura K, Dudley J, Nei M, Kumar S (2007) MEGA4: molecular evolutionary genetics analysis (MEGA) software version 4.0. Mol Biol Evol 24:1596–1599

Thomas Y, Bethenod MT, Pelozuelo L, Frerot B, Bourguet D (2003) Genetic isolation between two sympatric host-plant races of the European corn borer, *Ostrinia nubilalis* Hubner. I. Sex pheromone, moth emergence timing, and parasitism. Evolution 57:261–273

Tobin PC, Nagarkatti S, Loeb G, Saunders MC (2008) Historical and projected interactions between climate change and insect voltinism in a multivoltine species. Global Change Biol 14:951–957

Traut W, Marec F (1997) Sex chromosome differentiation in some species of Lepidoptera (Insecta). Chromosome Res 5:283–291

Vos P, Hogers R, Bleeker M, Reijans M, van de Lee T, Hornes M, Frijters A, Pot J, Peleman J, Kuiper M, Zabeau M (1995) AFLP: a new technique for DNA fingerprinting. Nucleic Acids Res 23:4407–4414

West-Eberhard MJ (2003) Developmental plasticity. Oxford University Press, USA, pp 553

Wolf KW (1996) The structure of condensed chromosomes in mitosis and meiosis of insects. Int J Insect Morphol Embryol 25:37–62

Wu Y, Close TJ, Lonardi S (2008) On the accurate construction of consensus genetic maps. CSB computational systems bioinformatics conference, Stanford, CA

Xia Q, Cheng D, Duan J, Wang G, Cheng T, Zha X, Liu C, Zhao P, Dai F, Zhang Z, He N, Zhang L, Xiang Z (2007) Microarray-based gene expression profiles in multiple tissues of the domesticated silkworm, *Bombyx mori*. Genome Biol 8:R162

Xiang H, Li M, Yang F, Guo Q, Zhan S, Lin H, Miao X, Huang Y (2008) Fine mapping of Ekp-1, a locus associated with silkworm (*Bombyx mori*) proleg development. Heredity 100:533–540

Yamamoto K, Narukawa J, Kadono-Okuda K, Nohata J, Sasanuma M, Suetsugu Y, Banno Y, Fujii H, Goldsmith MR, Mita K (2006) Construction of a single nucleotide polymorphism linkage map for the silkworm, *Bombyx mori*, based on bacterial artificial chromosome end sequences. Genetics 173:151–161

Yasukochi Y, Ashakumary LA, Baba K, Yoshido A, Sahara K (2006) A second-generation integrated map of the silkworm reveals synteny and conserved gene order between Lepidopteran insects. Genetics 173:1319–1328

Yasukochi Y, Tanaka-Okuyama M, Shibata F, Yoshido A, Marec F, Wu C, Zhang H, Goldsmith MR, Sahara K (2009) Extensive conserved synteny of genes between the karyotypes of *Manduca sexta* and *Bombyx mori* revealed by BAC-FISH mapping. PLoS ONE 4:e7465

Yokoyama T, Abe H, Irobe Y, Saito K, Tanaka N, Kawai S, Ohbayashi F, Shimada T, Oshiki T (2003) Detachment analysis of the translocated W chromosome shows that the female-specific randomly amplified polymorphic DNA (RAPD) marker, female-218, is derived from the second chromosome fragment region of the translocated W chromosome of the sex-limited p(B) silkworm (*Bombyx mori*) strain. Hereditas 138:148–153

Zha X, Xia Q, Duan J, Wang C, He N, Xiang Z (2009) Dosage analysis of Z chromosome genes using microarray in silkworm, *Bombyx mori*. Insect Biochem Mol Biol 39:315–321

Zhu Y, Chen P, Zhao T, Lu C, Xiang Z (2001) Research on the application of sch gene in the sex control of silkworm and the improvement of sex-limited male silkworm variety. Acta Sericologica Sin 27:253–256